AD-A118 895 AERONAUTICAL RESEARCH LABS MELBOURNE (AUSTRALIA) F/G 1/3
FLUTTER SUBSTANTIATION TESTS ON A TRANSAVIA PL-12/T-300 AIRTRUK--ETC(U)
JUN 82 A GOLDMAN
UNCLASSIFIED ARL/STRU-TM-341 NL

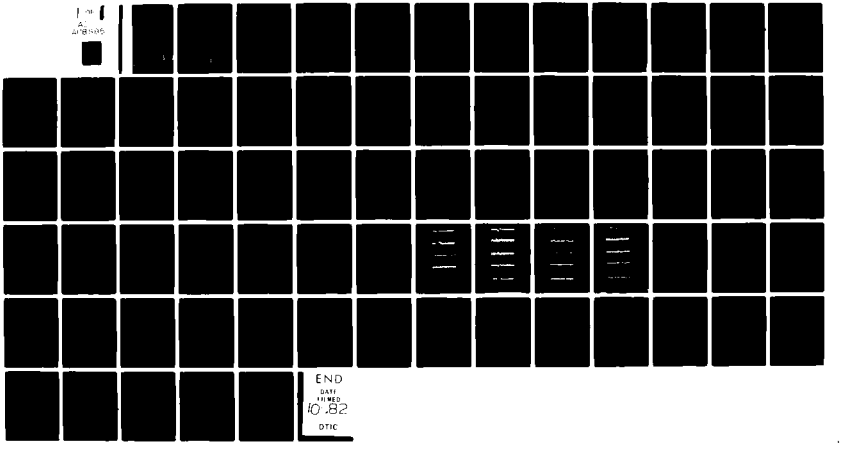

END
DATE FILMED
10-82
DTIC

(12)

ARL/STRUC-TECH-MEMO-341

AR-002-890

DEPARTMENT OF DEFENCE SUPPORT

DEFENCE SCIENCE AND TECHNOLOGY ORGANISATION

AERONAUTICAL RESEARCH LABORATORIES

MELBOURNE, VICTORIA

Structures Technical Memorandum 341

FLUTTER SUBSTANTIATION TESTS ON A TRANSAVIA FL-12/T-300 AIRTRUK

A. GOLDMAN

Approved for Public Release

JUNE, 1982

COPY No

DEPARTMENT OF DEFENCE SUPPORT
DEFENCE SCIENCE AND TECHNOLOGY ORGANISATION
AERONAUTICAL RESEARCH LABORATORIES

Structures Technical Memorandum 341

FLUTTER SUBSTANTIATION TESTS ON A TRANSAVIA PL-12/T-300 AIPTRUK

by

A. GOLDMAN

SUMMARY

A resonance test and subsequent flight tests have been conducted on a Transavia Airtruk. The natural modes and frequencies of vibration were measured in the ground tests, and attempts made to induce flutter during flight tests. The results of these tests are presented.

POSTAL ADDRESS: Chief Superintendent, Aeronautical Research Laboratories, P.O. Box 4331, Melbourne, Victoria, 3001, Australia.

CONTENTS

1. INTRODUCTION

The Transavia Airtruk has been in production for 10 years, more than 100 having been sold, and there is no record of loss due to structural failure in this time. In order to expand overseas markets, particularly in North America, full F.A.A. certification was required and the Aeronautical Research Laboratories were requested to assist with the flutter substantiation tests.

The aircraft has been frequently modified since the first production model and the aircraft tested was as detailed in Table 1, with major dimensions shown in Fig. 1(a). For the ground resonance tests, the aircraft was set up on partially inflated main wheels with the nose suspended, on a soft spring system, from the factory roof structure. With fuel tanks 50 per cent full and the hopper empty, the rigid body modes of pitch, roll, and heave were 1.4 hertz, 4.2 hertz and 4 hertz respectively.

The aircraft was complete and serviceable, with all components present in their correct locations.

The control surfaces were clamped to the main airframe for all the airframe modes except for the mode at 39.4 hertz, and freed for all the control surface measurements except tab rotation.

The undercarriage had the hydraulic dampers replaced with fixed struts, but the dampers were attached to the wheels to retain the correct mass distribution.

The same aircraft was used in the flight tests. All control cables were at the lower service limits of tension. No attempt was made to simulate in-service backlash increases.

2. TEST EQUIPMENT AND PROCEDURES

2.1 Ground Resonance Tests

A maximum of ten electro-magnetic vibrators was used for these tests. These vibrators were nominally identical having a maximum thrust of 138 newtons and diaphragm stiffness of approximately 5 kilonewtons/metre. The vibrators were initially located at the extremities of the wing front and rear spars, the port front spar and starboard rear spar of each tailplane, and in a horizontal direction at the lowest point of each fin.

The vibrators were mounted on adjustable height stands and attached to the aircraft structure through light-weight, telescopic rods using ball-jointed connectors bonded to the skin with a quick-setting adhesive. Relocation of vibrators was found to be necessary

for the wing torsion modes where the rear spar was very close to the nodal line, and for the control surface modes. For the wing torsion modes the two vibrators on the rear spars were relocated towards the wing trailing edges, and for the control surface modes vibrators were generally located at the trailing edge of the control surfaces.

The vibrators were driven by high output-impedance power-amplifiers to ensure that the applied forces were always in phase, irrespective of the motion of the structure. Frequency control was provided by a variable oscillator.

Accelerometers were located on the structure directly over each vibrator attachment and at six other locations, on the tailplanes and fins, to provide an indication of the phase of the response relative to the oscillator output signal. The sixteen accelerometer signals, and a signal from the oscillator in quadrature with the driving signal, were passed through a bank of phase-matched low-pass filters having a roll-off frequency of 45 hertz. This was to remove distortions in the signals caused by local panel resonances and other noise. The signals were then fed into a Resolved Component Ratiometer (RCR) and a multi-channel oscilloscope. The RCR operates by resolving each accelerometer signal into its components in phase and quadrature with a reference signal, summing the similar components, displaying the average value of in-phase and quadrature components, and displaying the ratio of the quadrature to the in-phase components of the response. Using a reference signal in quadrature with the forcing signal makes this ratio small at resonance. A pure resonant mode would provide a ratio of zero, whereas, if a reference was used in phase with the force, the ratio would approach infinity and overload the display of the ratiometer.

Likewise, the use of the quadrature reference signal provides Lissajous figures on the oscilloscope which are straight lines at resonance. Use of a signal in phase with the force would provide circles at resonance, which would make tuning rather difficult.

As an aid to determination of the resonant frequencies of the airframe, a random noise signal, of bandwidth 0 to 50 hertz, was fed into a vibrator at three consecutive locations - wing tip, tail-plane tip, and fin tip. The response of the accelerometer directly over the vibrator was analysed, together with the random signal, on a dual-channel real-time spectrum analyser. In Fig. 2 the transfer function of response, with reference to random input, is displayed and the peaks annotated with the modes that were subsequently found close to the frequencies indicated. The only modes found which did not show up on these responses were wing torsion, and some of the boom bending and torsion modes. At each of the resonant frequencies indicated by the spectrum analyser, the force levels in all the

vibrators were manually adjusted until the acceleration responses at all the monitoring stations were as close as possible to being in quadrature with the exciting force. This was determined by observation of the Lissajous figures, and the RCR display, to obtain a condition with all figures as close as possible to straight lines, and the ratio displayed being a minimum. With a complex structure it is generally not possible, with a limited number of force inputs, to obtain a pure resonant mode.

Modes were found at all the frequencies indicated on the spectrum analyser. Other modes were found at frequencies not indicated initially. Modal measurements were made with a single movable accelerometer attached to the structure, by a suction cup, successively at each point of the array of measuring stations. The layout of the measurement points on the aircraft is indicated in Fig. 1(b) in which half the aircraft is shown. The distribution of measurement points was symmetrical about the centre line. The actual locations are listed and dimensioned in Table 2.

The accelerometer signal was fed to a digital transfer function analyser, which displayed the in-phase and quadrature components of the response with reference to the forcing signal. Modal damping measurements were obtained from records of the decay rates of the vibration when the exciting signal from the oscillator was disconnected.

On completion of the airframe vibration mode measurements, the vibrators were disconnected from the structure, and the control surfaces freed by removing all clamps. The airframe was then rigidly supported at the wings, booms and tailplanes using contour boards on stands with the airframe held onto them with bags of sand. This was done to permit measurement of the uncoupled control surface modes. Accelerometers and vibrators were relocated to suit the individual control surfaces, and resonant modes excited as before, using random input and the spectrum analyser to detect resonances. The oscillator was then used to fine-tune each resonant vibration mode. The aileron, elevator and rudder resonances were obtained by attaching one or more vibrators to the trailing edges of the respective control surface. The tab rotational frequencies were obtained by clamping the elevator to the tailplane and attaching the vibrator to the elevator. The only attachment to the tab was an accelerometer on the trailing edge. A random signal was fed into the vibrator and the transfer function of the tab was determined on the spectrum analyser for the three positions of each tab. The tabs are of the spring loaded type.

The elevator control is connected to a downspring which holds the control column in a full forward position when released. To hold the column central required several restraining rubber cords. The test on the elevators was repeated with a single rubber cord on the control column to try and simulate a hand held situation, and also with the downspring removed completely.

2.2 Flight Tests

Lightweight accelerometers, having a mass of 8 grams each, were fixed to the aircraft structure at thirteen locations as listed in Table 3. Wherever possible, the accelerometers were fixed inside the structure. The accelerometers on the elevator and rudder were mounted externally. In all locations the accelerometers were fixed to the structure with a quicksetting epoxy resin adhesive. On the external surfaces they were also faired with tape to improve airflow. Cables were run, under covers and along wing trailing edges, to amplifiers located in the passenger compartment. This compartment also housed the power supplies, DC to AC invertor, and a 14-track instrumentation tape-recorder. A remote control station and microphone were installed in the pilot's compartment.

Two test flights were made, to cover a total of 12 test points. This involved making several dives from approximately 3400 metres to 1200 metres altitude and holding each required airspeed steady while the control stick was sharply struck in both fore and aft, and sideways directions, to induce a sudden disturbance on the surfaces. The test points, and air speeds are listed in Table 4.

The records were replayed into a multi-channel chart recorder to observe the actual time histories at each test point. In order that the traces were not swamped by noise signals outside the range of interest, the signals were passed through a bank of low-pass filters having a roll-off at 45 hertz. Samples of this time history are presented in Fig.15.

To investigate the frequency response of the structure to the general turbulence present at different speeds the recorded data were analysed on a Fourier analyser, two channels at a time. The spectra obtained for the speeds of 145 and 175 knots are presented in Figs. 16 to 18. In order to obtain the impulse response of the structure, the Random Decrement procedure was used. This procedure is based on methods described in Ref. 1. Two techniques were used to produce Figs 19 to 22 which illustrate the random decrement signatures at different parts of the structure. Initially, the data were passed through a low-pass filter set successively at 10, 15, 20, 25 and 30 hertz to examine responses in each of these ranges, the highest frequency present being dominant in each case. The signal was then digitised at a rate of 1000 samples per second and passed through a microprocessor to provide an acceleration decrement signature of 0.5 seconds duration. Fig. 22 is the only figure presented which used this technique. The results at the lower frequencies were distorted due, it is thought, to the poor cut-off characteristics of the analogue filters used, and the closeness of various vibration frequencies. To improve matters, digital filters were used after the analogue data had been digitised at the rate of 1280 samples per

second using a time history 1.6 seconds long. At each test point and location three such time histories were used to provide the data which were then analysed using a random decrement programme on a DEC PDP-10 computer to produce Figs. 19 to 21.

3. TEST RESULTS

3.1 General

The vibration mode shapes for all the measured flexible modes are listed in Table 5 and plotted in Figs. 3 to 14. In all instances only the response of the structure in quadrature with the exciting force is plotted. For clarity of presentation, not every measured point is plotted, and in cases where the vibration amplitudes on certain components of the aircraft structure were negligible, measurements were not recorded.

3.2 Details of Mode Shapes

Mode at 5.14 Hz. (Fig. 3)

This mode is the antisymmetric lateral bending of the booms. Because of the high tailplane some torsion is also introduced. There is also slight antisymmetric bending of the wings.

Mode at 6.07 Hz. (Fig. 4)

This is antisymmetric vertical bending of the booms. The motion of the wings is essentially rigid body motion.

Mode at 9.7 Hz. (not illustrated)

This is the rotation frequency of the elevators. The control spring had been removed and a rubber cord was used to hold the control column central. It was considered that this best simulated actual flying conditions. The response of each elevator was independant of the other and could be made to oscillate in-phase or in opposition.

Mode at 9.9 Hz. (Fig. 5)

This is symmetric torsion of the booms. The two booms are slightly different, and with the close proximity of the antisymmetric mode at 10.5 Hz some difficulty was experienced initially in separating the two modes.

Mode at 10.5 Hz. (Fig. 6)

This is the antisymmetric torsion mode of the booms. This mode was excited mainly by forces on the starboard tail with a slight restrainin

force on the front tail whereas the mode at 9.9 Hz. was excited solely from forces on the port tail. The main wing is indicating symmetric bending in spite of the antisymmetric nature of the reaction torque applied at the boom connection. This is no doubt due to the close proximity of the fundamental wing bending mode at 11.4 Hz.

Mode at 11.4 Hz. (Fig. 7)

This is fundamental wing bending coupled with symmetric boom torsion. The boom torsion is the main cause of the sharp change in bending at the intersection of boom and wing.

Mode at 14.2 Hz. (not illustrated)

This is elevator rotation with the control column fixed. The column, with its control spring, was lashed in two directions using rubber cords. The damping measured in this mode is quite high; in excess of 5 percent of critical damping. The elevator rotation could be in-phase or anti-phase depending upon direction of force input. This mode appears very similar to the mode at 9.7 hertz.

Mode at 14.4 Hz. (Fig. 8)

This is the wing antisymmetric bending mode. Antisymmetric bending of the booms occurs with rotation of tailplanes.

Mode at 21.6 Hz. (not illustrated)

This is anti-phase rotation of the two rudders with the control column free. This mode was excited with a force on the port rudder only.

Mode at 23.4 Hz. (not illustrated)

This is symmetric rotation of the ailerons with the stick free.

Mode at 30.8 Hz. (not illustrated)

This is the symmetric bending of the stub wing, and was excited via force inputs to the main wings.

Mode at 35.6 Hz. (Fig. 9)

This is the symmetric wing torsion mode coupled with spanwise aileron bending.

Mode at 38 Hz. (Fig. 10)

This mode is essentially rudder bending about its hinge line, coupled with antisymmetric tailplane torsion. The rudder was clamped to the fin at the hinge line with a single clamp. The tailplane torsion is present because of the close proximity of the mode at 38.4 Hz. measured with the control surfaces free.

Mode at 38.4 Hz. (Fig. 11)

This is antisymmetric torsion of the elevator.

Mode at 39.4 Hz. (Fig. 12)

This mode is antisymmetric wing torsion and antisymmetric aileron torsion coupled with aileron bending. This mode was measured with the ailerons free to rotate and with the airframe on its soft support.

Mode at 43.2 Hz. (Fig. 13)

This is rudder bending coupled with some boom torsion which causes the tailplane to roll.

Mode at 46.5 Hz. (Fig. 14)

This mode is symmetric tailplane bending.

Mode at 48 Hz. (not illustrated)

This is the rotation frequency of the tailplane tab when in the maximum down position.

Mode at 53.6 Hz. (not illustrated)

This is the rotation frequency of the tailplane tab when in the mean position.

Mode at 55.2 Hz. (not illustrated)

This is the rotation frequency of the tailplane tab when in the maximum up position.

3.3 Flight Tests

On the samples of time history produced in Fig. 15 the impulses applied to the ailerons are well defined, as are the responses on the wings and boom to the impulses. The impulses applied to the elevators are not obvious no doubt due to the damping effect of the long control

cables, which pass over several pulleys and two 90 degree changes in direction before reaching the elevator. The general level of random acceleration at the elevator, as measured by the accelerometers and shown in Figs. 15(b) and 15(d), is almost equal in amplitude to the impulses applied to the ailerons, and should have been sufficient to initiate flutter if the aircraft had crossed a flutter boundary. It should be noted that the vertical scale used in Figs. 15(c) and 15(d) is 10 times that used in Figs. 15(a) and 15(b). The accelerometer amplifier sensitivity was also changed following the first flight, as saturation of the amplifiers was suspected. The top record on Fig. 15(d) indicates that saturation was a problem with that particular amplifier even at the lower sensitivity. Figs. 16 to 18 show the frequency spectra of the accelerations at six locations and two air speeds. The most significant feature appears on Figs 16(a) and 16(b) where a sharp peak can be seen at approximately 21 hertz on both wing and aileron.

Detailed investigation of the records at other speeds and altitudes indicates that the vibration frequency and amplitude does not vary between speeds from 100 to 175 knots, or altitudes from 1230 to 2770 metres, and generally does not exceed 1 millimetre peak-to-peak at the aileron trailing edge. The oscillation disappeared at various times during the flights, particularly at times when the pilot may have been undertaking manouvres using the ailerons.

In Figs. 19 to 21 (produced by Random Decrement Analysis), which indicate the impulse response of the structure at six locations at a speed of 175 knots, it can be seen that vibrations around the tail region are damped. In Fig. 20(a) the wing and aileron show a relatively low damped oscillation at 10 hertz. This is due to leakage of the response of the wing bending mode of about 12 hertz, (see Fig. 16(a)), through the filter at 10 hertz. Fig. 20(b) shows this mode correctly at about 12 hertz with higher damping.

Fig. 20(d) shows the aileron having signs of a lightly damped oscillation in the 20 to 25 hertz range. To illustrate the aileron vibration further, Fig. 22 is presented to show the rapid decay from the initial peak response to the continuing limited amplitude oscillation. The two curves indicate that the frequency and damping of the aileron oscillation is independent of air speed in the range covered by the test.

4. DISCUSSION

The approach to determining the resonant frequencies of the structure by use of a spectrum analyser appears to have some shortcomings. The method adopted in this test, of using a random input and a transfer function of the response with reference to the input,

generally showed the regions in which resonances occurred, but was unable to separate close resonances, such as the symmetric and antisymmetric boom torsion modes, even when using the band expansion capabilities of the analyser. However, the frequency spectra shown in Fig. 2 indicate all the regions in which there were airframe vibration modes except the wing torsion modes. This omission was caused by placing the accelerometer and shaker close to the torsional nodal line. This would have been avoided if the wing-tip leading-edge had been used.

With the flight tests, the fact that the pilots cabin and theinstrumentation compartment were well separated introduced the problem of monitoring the operation of equipment in flight. It is apparent that a telemetry system, with remote control of amplifier gains, would be an advantage in this type of work. This would also obviate the need to carry the tape recorder on the flight.

5. CONCLUSIONS

The aircraft has been ground tested, in relation to its airframe vibration characteristics, and all the expected modes of vibration measured. The flight tests have been carried out and every reasonable effort made to induce flutter at speeds up to 175 knots. The aircraft, in the configuration tested, has been found to be clear of flutter at air speeds up to and including 175 knots.

REFERENCES

1. H.A. Cole. On-line failure detection and damping measurement of aerospace structures by Random Decrement signatures.
NASA CR-2205, 1973.

TABLE 1(a)

DETAILS OF AIRCRAFT FOR GROUND RESONANCE TEST

Aircraft type:	Transavia PL-12/T-300 Airtruk
Serial No.:	G996
Registration:	VH-UOT
Engine:	Lycoming Type IO-540-K1AS Serial No: L-18871-48A
Propeller.	Hartzell Type HC-C3YR-1RF/F8468A-2R Serial No: DY903
Hopper configuration:	Wet/Dry Doors
Flap Control:	Standard manual

Modifications incorporated:

No. 140	Horn balance elevators
No. 141	Bevel Trailing Edge Ailerons
No. 143	Elevator Down Spring

Total mass approx. - 1000 kilograms

Centre of Gravity approx. - 420 millimetres aft of main wing leading edge.

TABLE 1(b)

AIRCRAFT CONFIGURATION FOR FLIGHT TESTS

Mass of aircraft plus oil, fuel, pilot, parachute, battery pack, tape recorder, amplifiers, etc.	1408 kilograms
Maximum permitted mass of aircraft	1742 kilograms
Centre of Gravity of aircraft at take-off.	0.532 metres aft of datum
Limits of Centre of Gravity	0.417 to 0.589 metres aft of datum
Moment about Centre of Gravity	7350 Newton-metres

Control surface balances:-

Trim tab	0.3 kilograms T.E. heavy
Elevator	0.14 kilograms L.E. heavy
Aileron	1.59 kilograms T.E. heavy
Rudder	0.75 kilograms T.E. heavy

TABLE 2(a)

LOCATION OF WING MEASURING STATIONS

η \ ξ	0.015	0.202	0.635	0.765	0.995
+0.995	-	W1B	W1C	W1D	-
-0.995	-	W12B	W12C	W12D	-
+0.844	W2A	W2B	W2C	W2D	W2E
-0.844	W11A	W11B	W11C	W11D	W11E
+0.665	W3A	W3B	W3C	W3D	W3E
-0.665	W10A	W10B	W10C	W10D	W10E
+0.470	W4A	W4B	W4C	-	W4E
-0.470	W9A	W9B	W9C	-	W9E
+0.318	W5A	W5B	W5C	W5D	W5E
-0.318	W8A	W8B	W8C	W8D	W8E
+0.131	W6A	W6B	W6C	W6D	W6E
-0.131	W7A	W7B	W7C	W7D	W7E

ξ is proportion of wing chord aft of wing leading edge

η is proportion of wing semi-span from aircraft centreline

TABLE 2(b)

LOCATION OF TAILPLANE MEASURING STATIONS

η \ ξ	0.042	0.375	0.625	0.986
+ 0.875	PT1A, ST1A	PT1B, ST1B	PT1C, ST1C	PT1D, ST1D
- 0.875	PT4A, ST4A	PT4B, ST4B	PT4C, ST4C	PT4D, ST4D
+ 0.484	PT2A, ST2A	PT2B, ST2B	PT2C, ST2C	PT2D, ST2D
- 0.484	PT3A, ST3A	PT3B, ST3B	PT3C, ST3C	PT3D, ST3D

ξ is proportion of tailplane chord aft of tailplane leading edge.

η is proportion of tailplane semi-span from boom centreline.

TABLE 2(c)

LOCATION OF FIN, RUDDER AND BOOM MEASURING STATIONS

W.L. \ B.S.	2640	3810	4220	4440	4950
- 305			PF4A SF4A	PF4B SF4B	PF4C SF4C
- 75				PF3B SF3B	PF3C SF3C
0	PB1H, SB1H PB1V, SB1V	PB2H, SB2H PB2V, SB2V			
+ 355			PF2A SF2A	PF2B SF2B	PF2C SF2C
+510			PF1A SF1A	PF1B SF1B	PF1C SF1C

B.S. - Body Station in millimetres from main wing root leading edge.

W.L. - Water line in millimetres from boom centreline.

TABLE 3

LOCATION OF ACCELEROMETERS FOR FLIGHT TESTS

Port aileron - measuring station W11E

Port-wing fron spar - measuring station W11B

Port-wing rear spar - measuring station W11C

Starboard-wing front spar - measuring station W2B

Starboard-wing rear spar - measuring station W2C

Port fin - measuring station PF2B

Port fin - measuring station PF4B

Port boom - 0.5 metres aft of PB2V

Port tailplane - inboard of PT1B

Port elevator - measuring station PT4D

Port elevator - measuring station PT1D

Port rudder - measuring station PF2C

Port rudder - measuring station PF4C

(Refer Fig. 1(b) for locations of measuring stations)

TABLE 4

FLIGHT TEST POINTS

Test point	I.A.S. Knots	Altitude metres(feet)	Date flown
1	106	2770 (9000)	10th July 1981
2	117	2000 (6500)	10th July 1981
3	128	1230 (4000)	10th July 1981
4	128	2770 (9000)	10th July 1981
5	138	2000 (6500)	10th July 1981
6	148	1230 (4000)	10th July 1981
7	145	2770 (9000)	12th July 1981
8	152	2000 (6500)	12th July 1981
9	160	1230 (4000)	12th July 1981
10	160	2770 (9000)	12th July 1981
11	166	2000 (6500)	12th July 1981
12	175	1230 (4000)	12th July 1981

TABLE 5

SUMMARY OF MEASURED MODES

Description of Mode	Natural Frequency Hz	Damping % Critical	Ratiometer Rdg. Q/R	Fig. No.
Antisymmetric lateral bending of booms	5.14	2.2	0.26	3
Antisymmetric vertical bending of booms	6.07	2	0.05	4
Elevator rotation - stick free and downspring removed	9.7	-	-	N.I.
Symmetric torsion of booms	9.9	-	0.07	5
Antisymmetric torsion of booms	10.5	1.7	0.08	6
Symmetric wing bending with symmetric boom torsion	11.4	1	0.08	7
Elevator rotation - stick fixed	14.2	>5	-	N.I.
Antisymmetric wing bending with antisymmetric boom torsion	14.4	2.9	0.05	8
Rudder anti-phase rotation - stick free	21.6	-	-	N.I.
Aileron symmetric rotation	23.4	2.4	-	N.I.
Stub wing symmetric bending	30.8	-	-	N.I.
Symmetric wing torsion with aileron bending	35.6	2.5	0.2	9
Rudder bending with tailplane antisymmetric torsion	38	2.2	0.15	10
Elevator antisymmetric torsion	38.4	1.4	-	11
Antisymmetric wing torsion and antisymmetric aileron torsion with aileron bending	39.4	2.4	-	12
Rudder bending	43.2	1.5	0.11	13
Symmetric tailplane bending	46.5	1.8	0.1	14
Tab rotation - max. down position	48	-	-	N.I.
Tab rotation - mean position	53.6	-	-	N.I.
Tab rotation - max. up position	55.2	-	-	N.I.

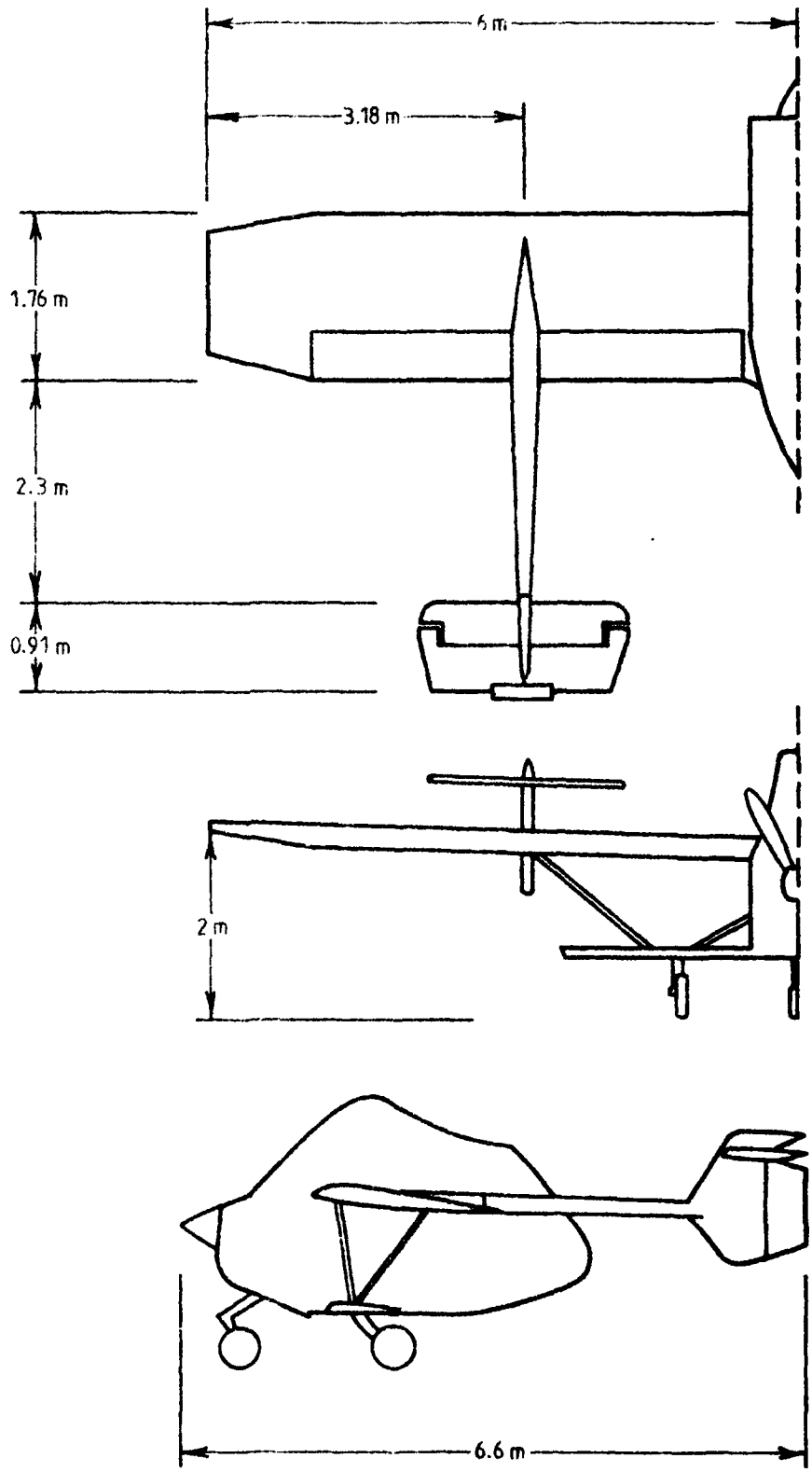

FIG.1(a) GENERAL OUTLINE OF AIRCRAFT WITH MAJOR DIMENSIONS

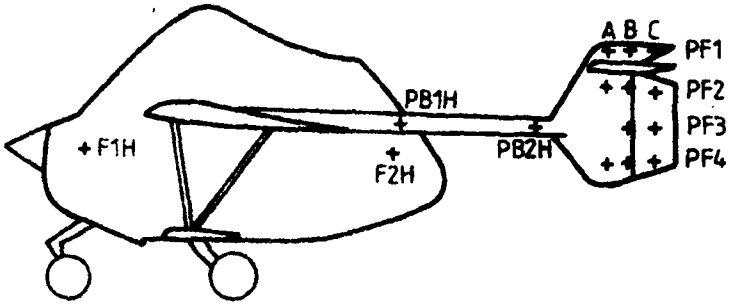

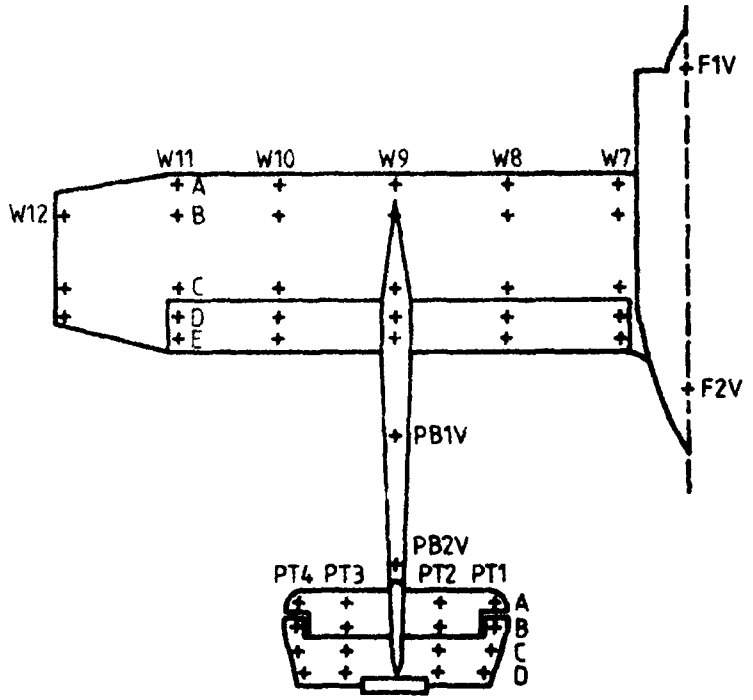

FIG.1(b) LOCATIONS OF MEASURING STATIONS (only half shown here)

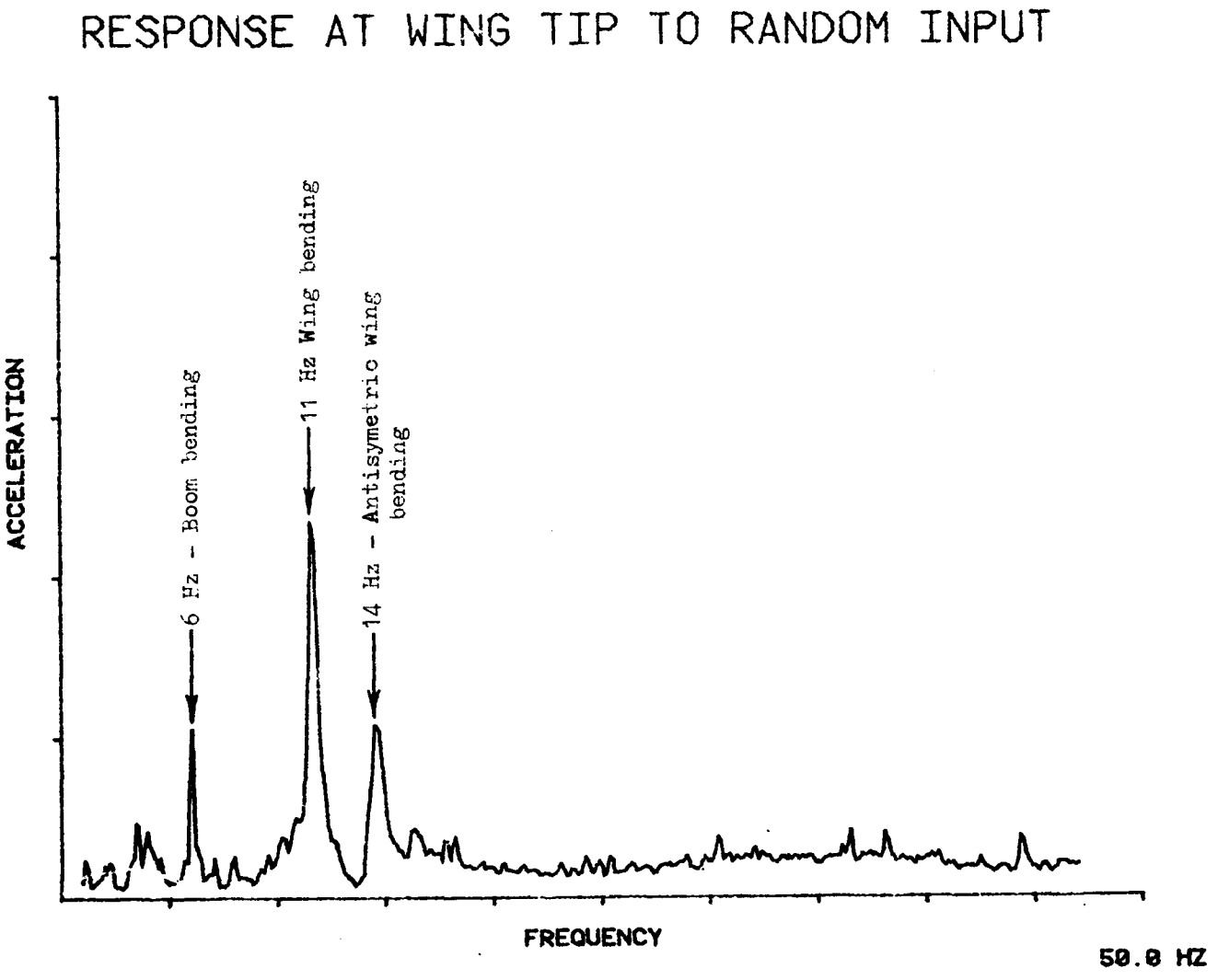

FIG.2(a) RESPONSE TO RANDOM INPUT

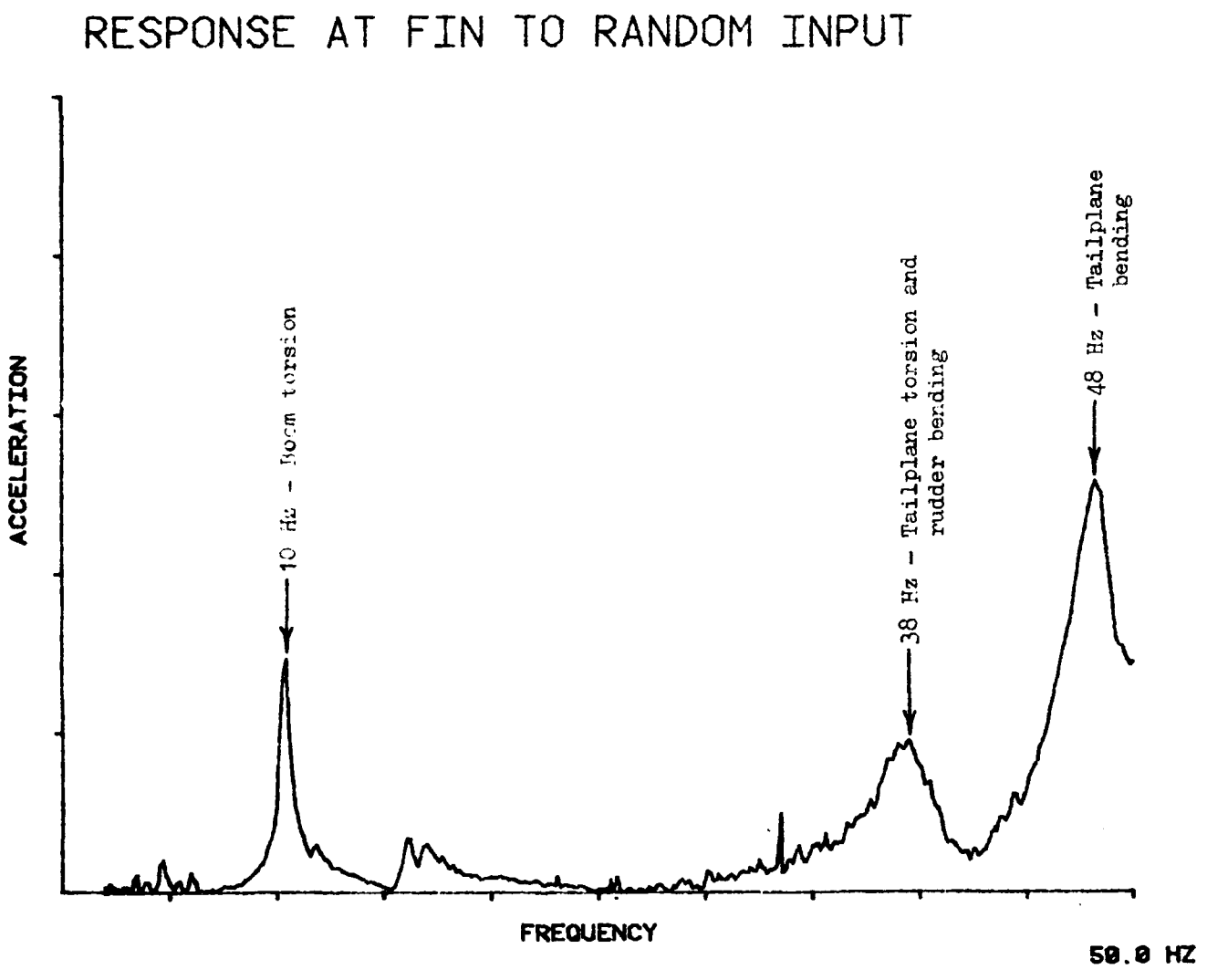

FIG.2(b) RESPONSE TO RANDOM INPUT

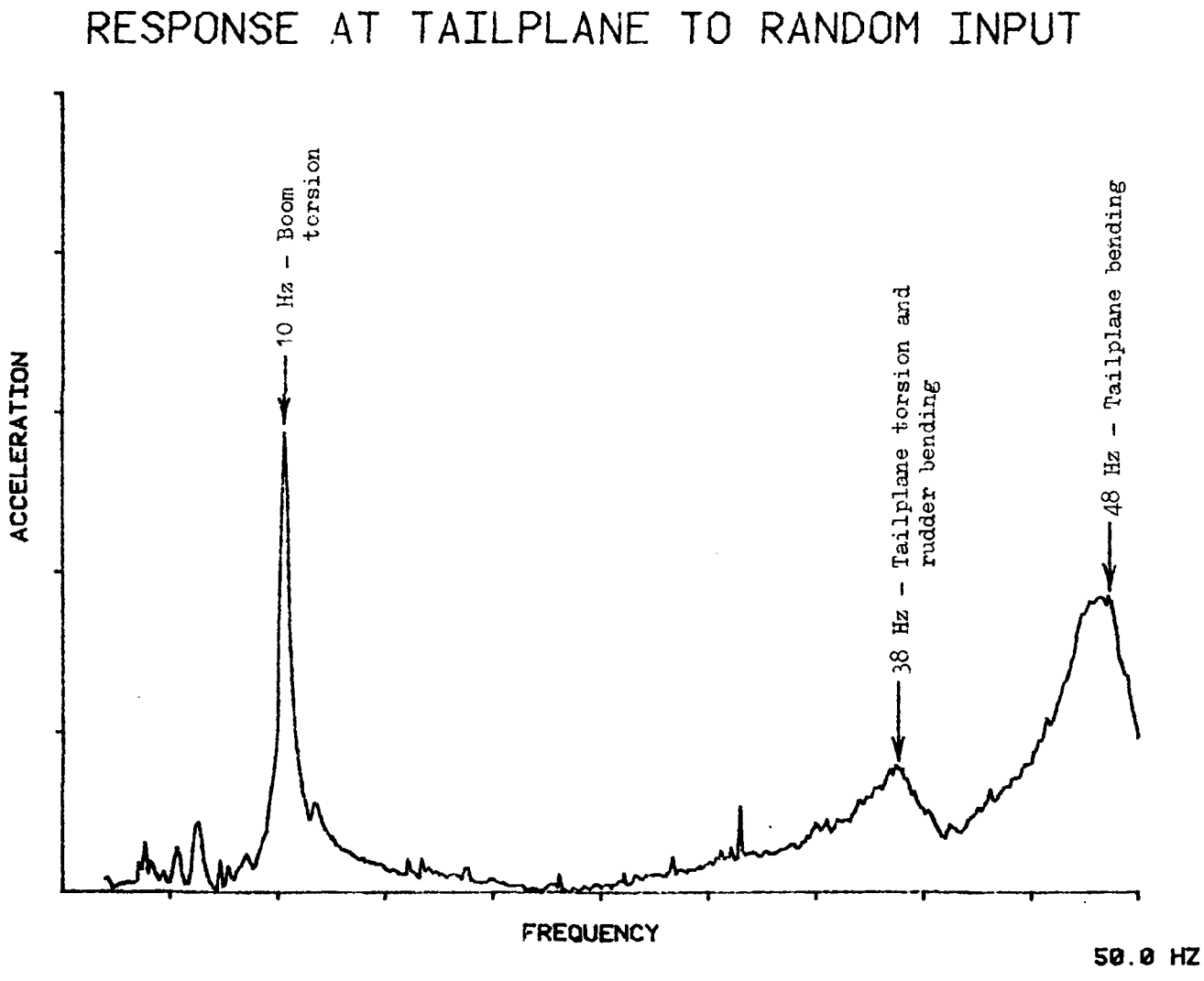

FIG.2(c) RESPONSE TO RANDOM INPUT

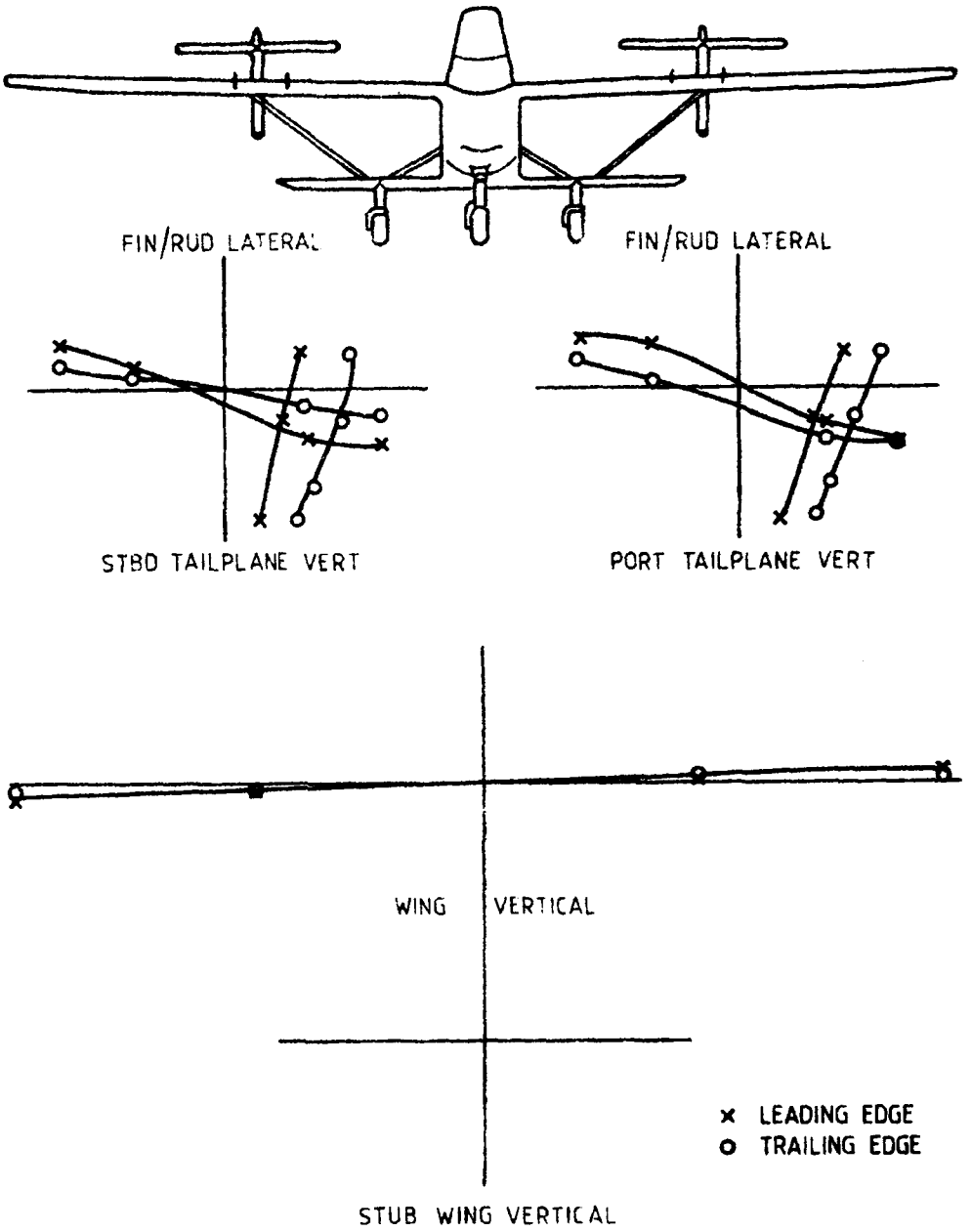

FIG.3(a) MODE AT 5.14 Hz

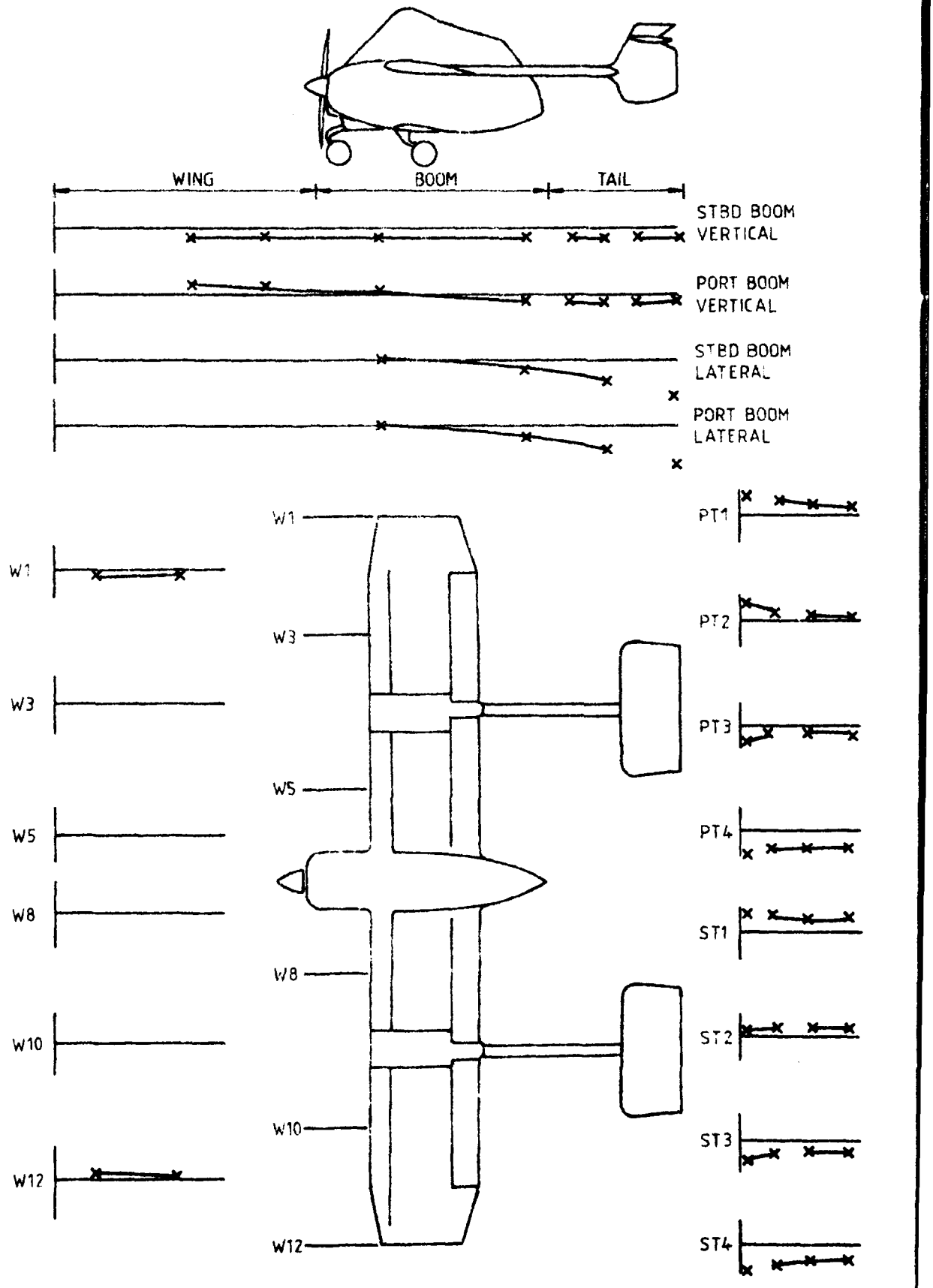

FIG. 3(b) MODE AT 5.14 Hz

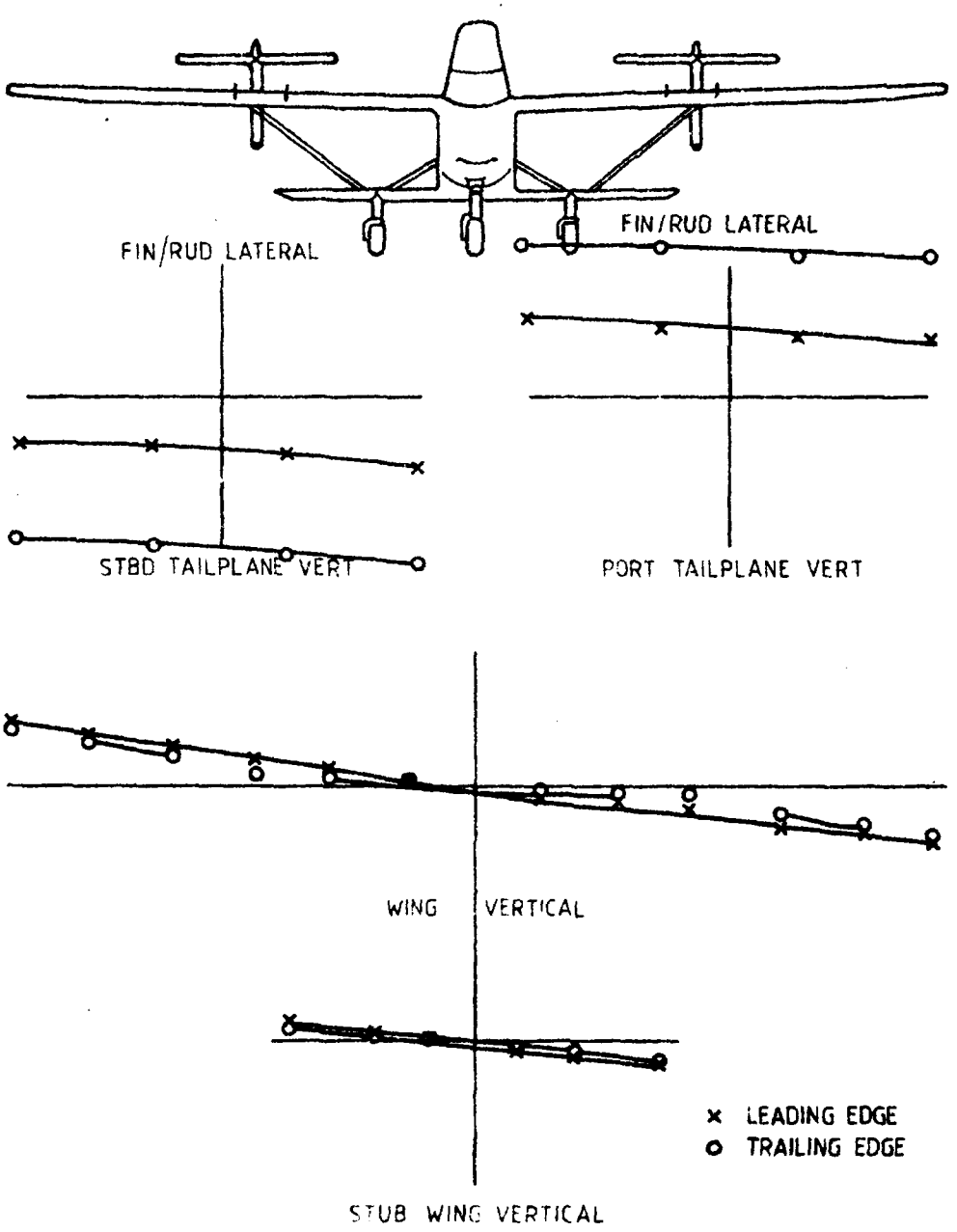

FIG.4(a) MODE AT 6.07 Hz

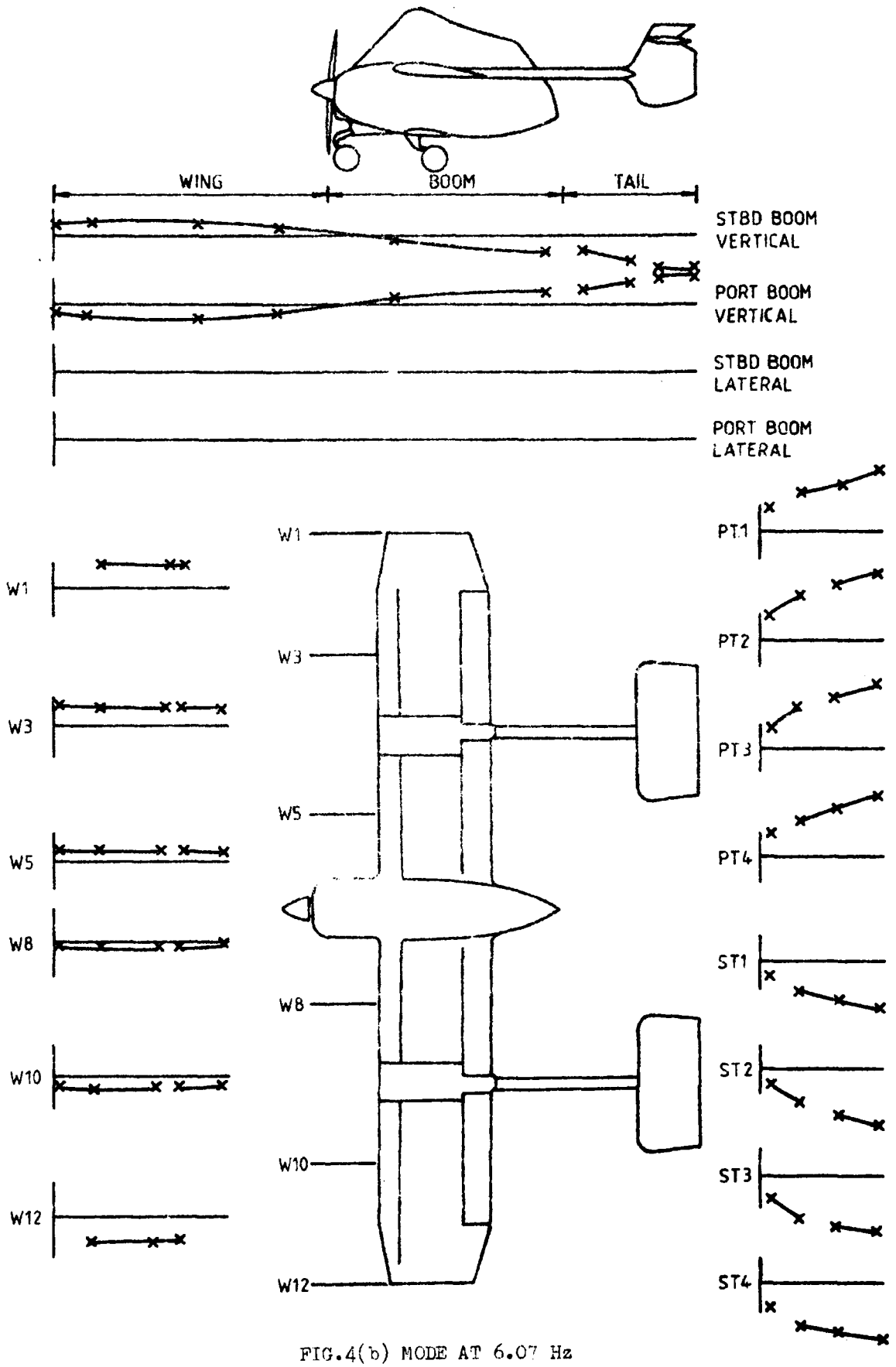

FIG.4(b) MODE AT 6.07 Hz

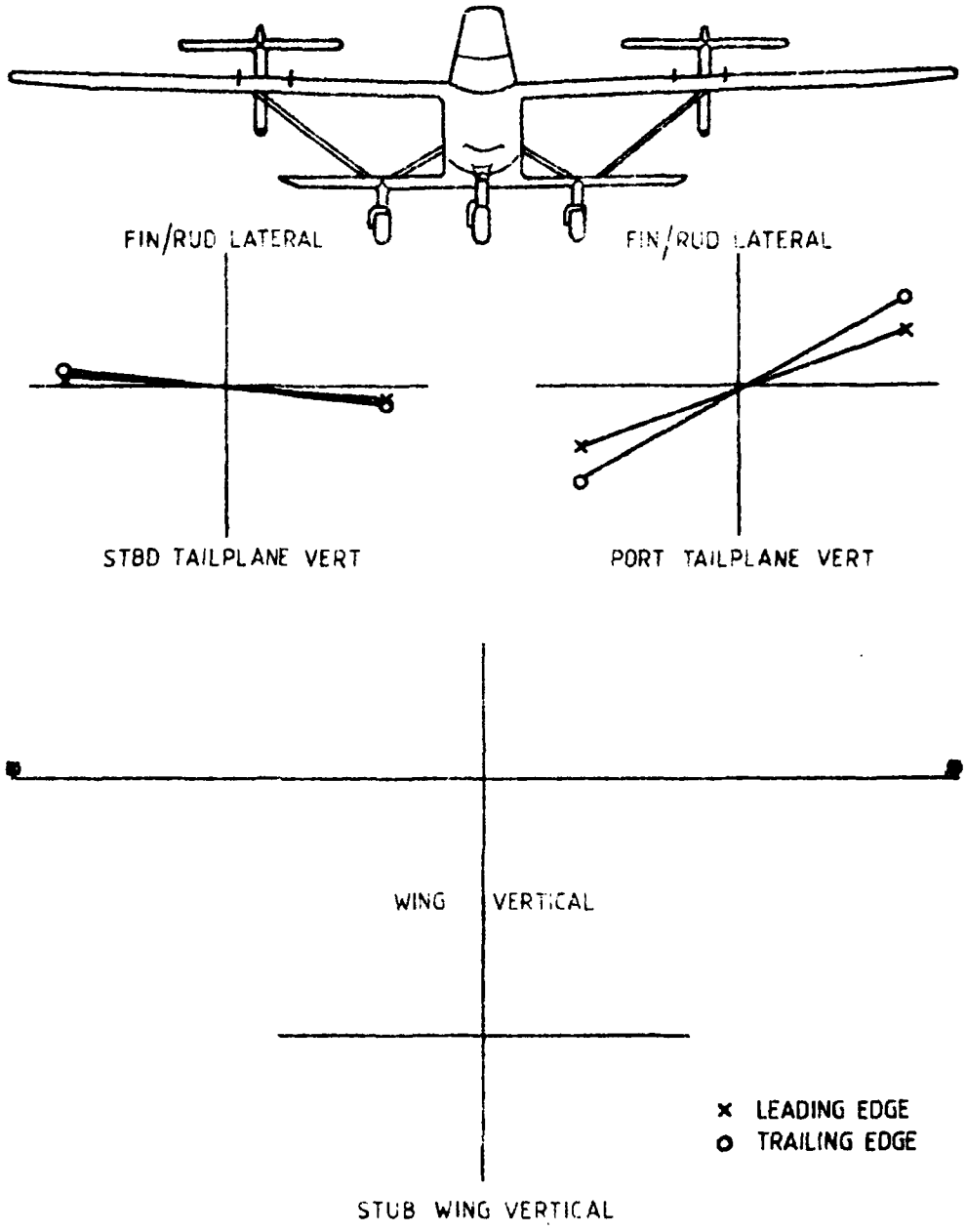

FIG.5(a) MODE AT 9.9 Hz

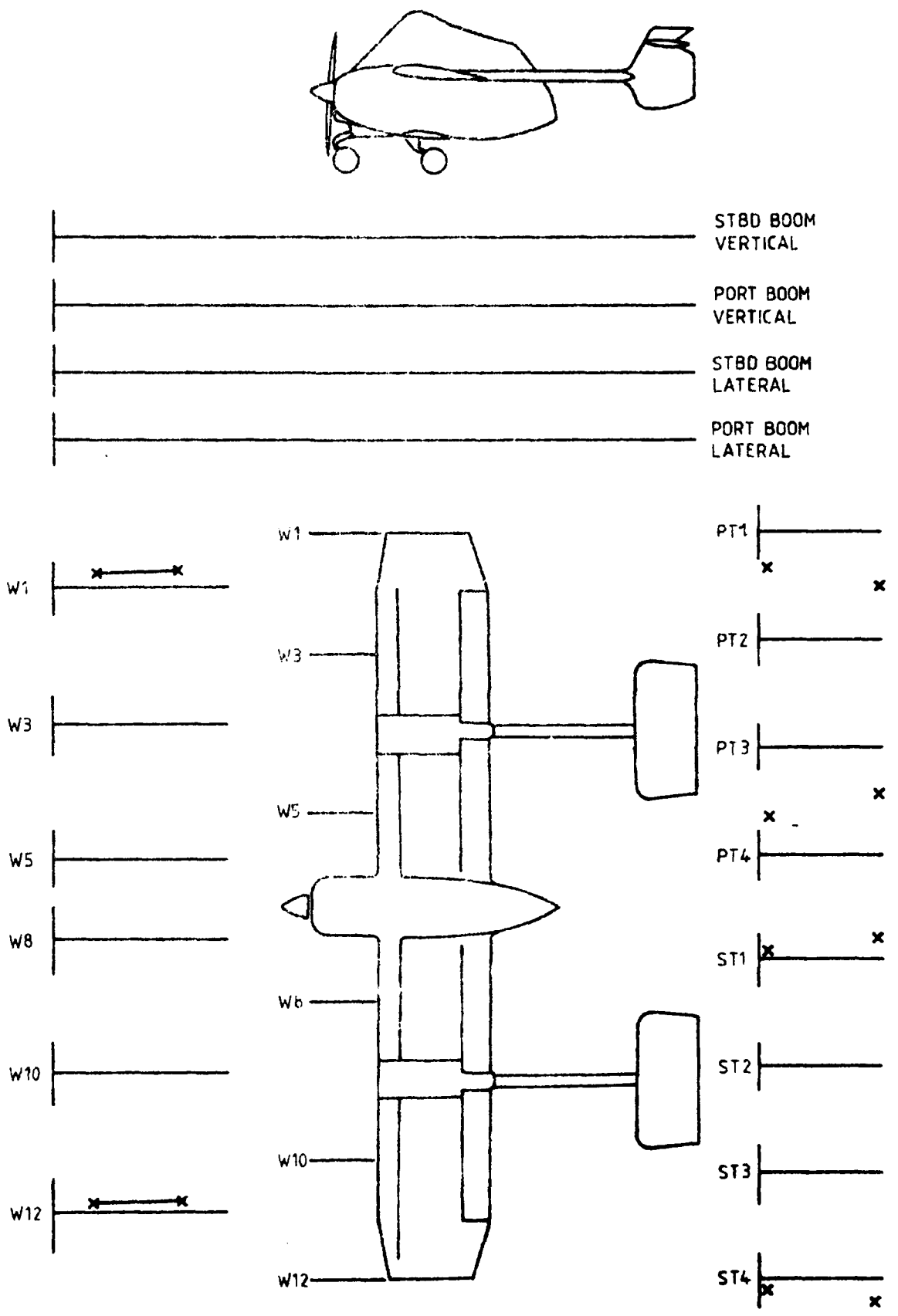

FIG.5(b) MODE AT 9.9 Hz

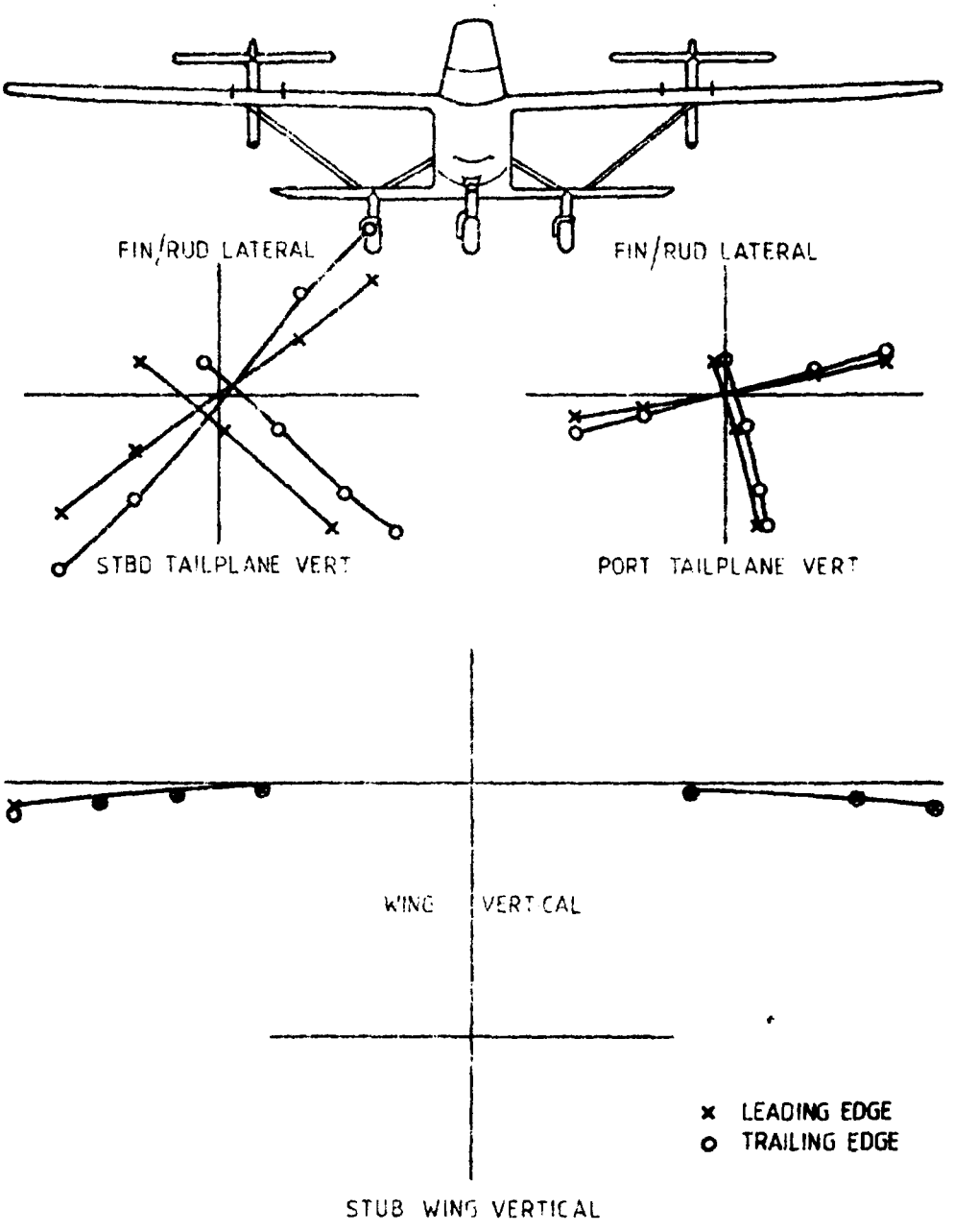

FIG.6(a) MODE AT 10.5 Hz

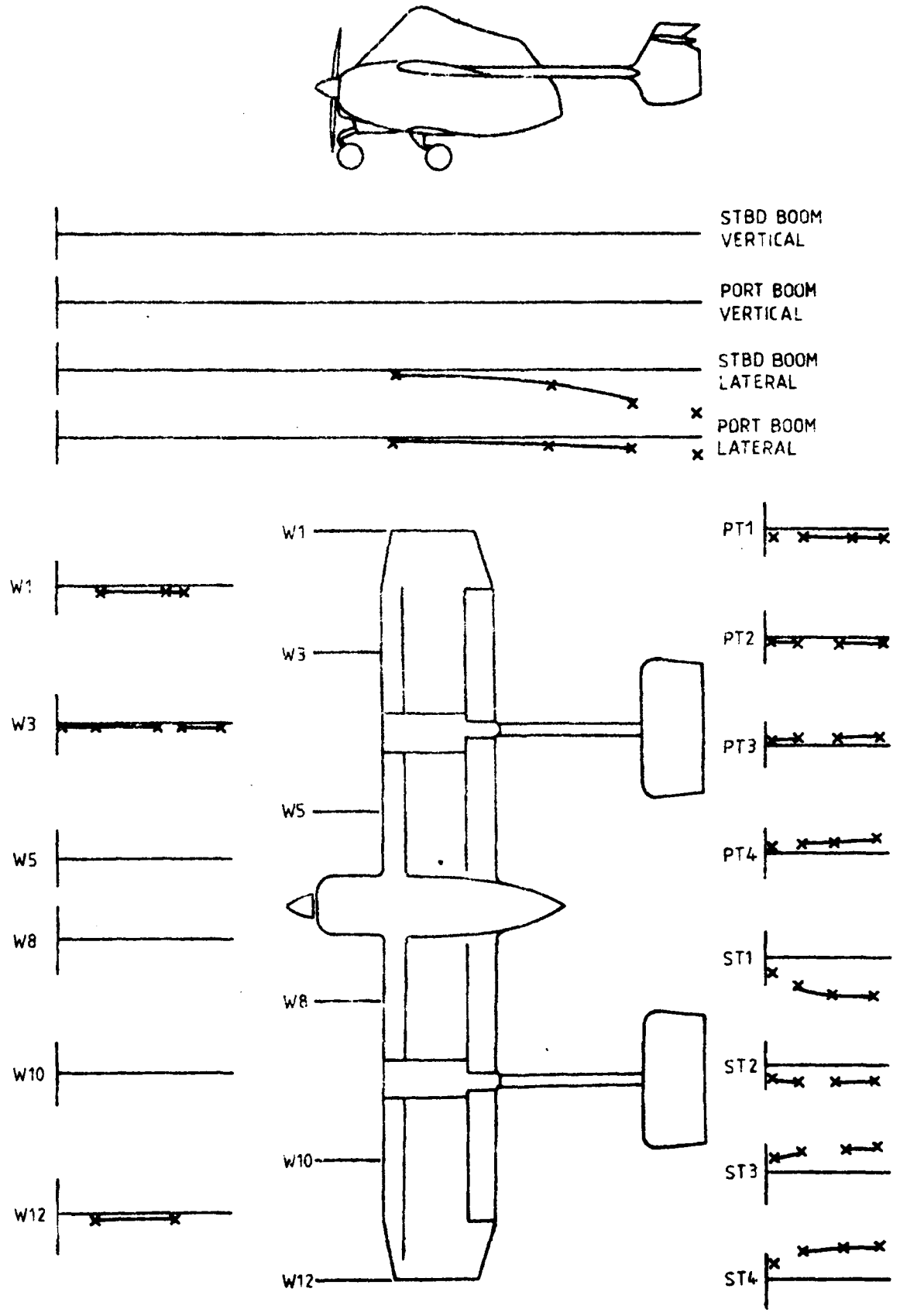

FIG.6(b) MODE AT 10.5 Hz

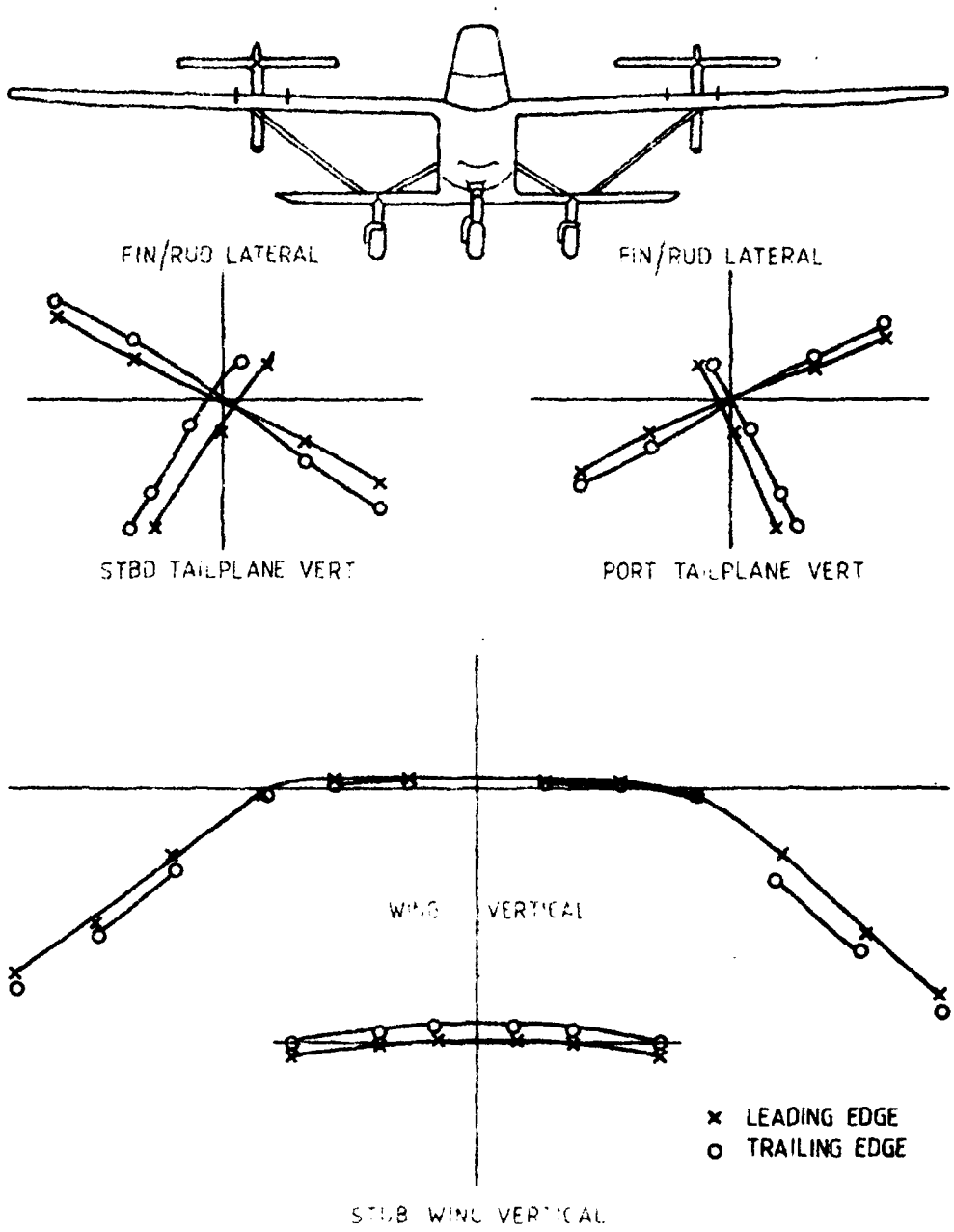

FIG.7(a) MODE AT 11.4 Hz

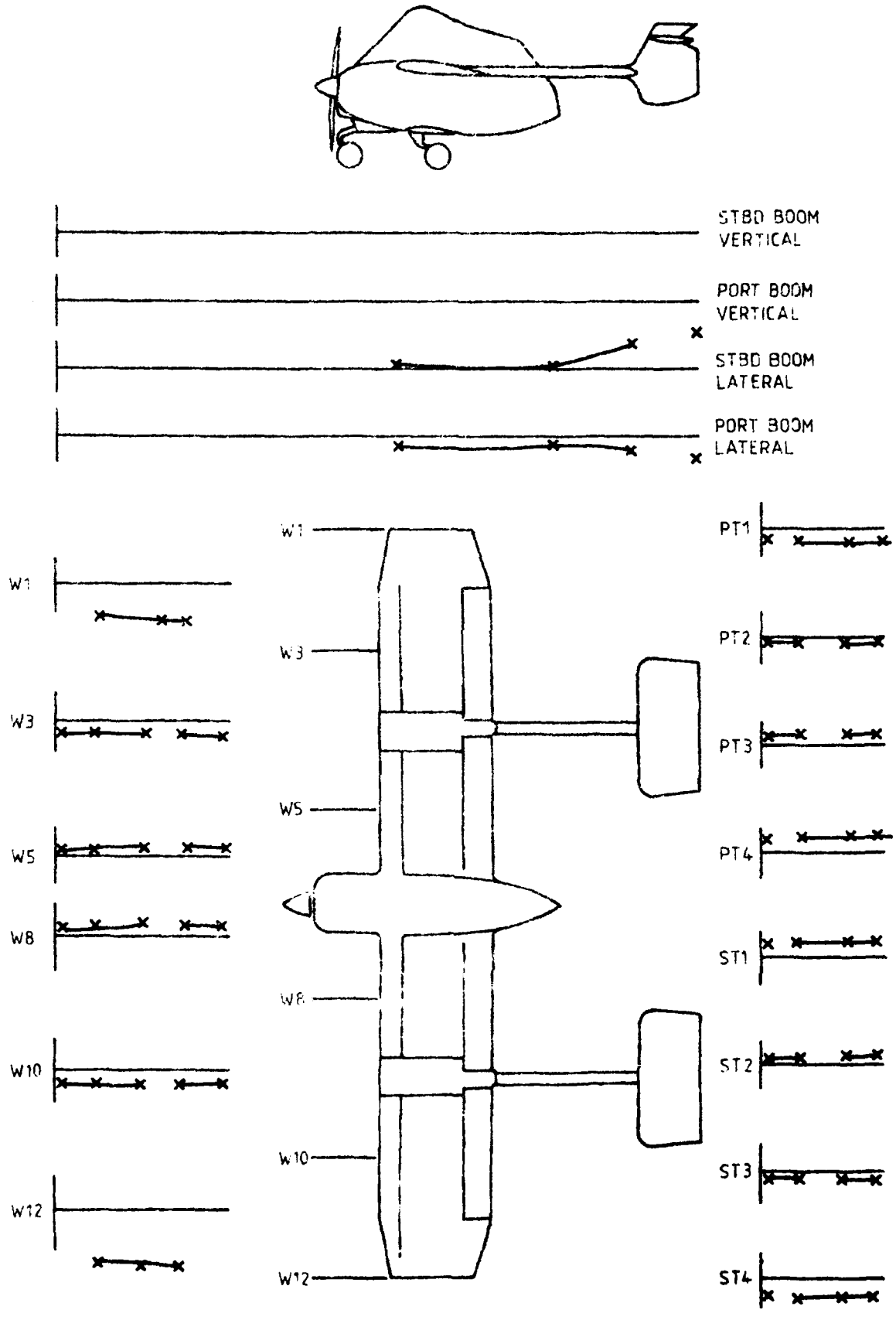

FIG.7(b) MODE AT 11.4 Hz

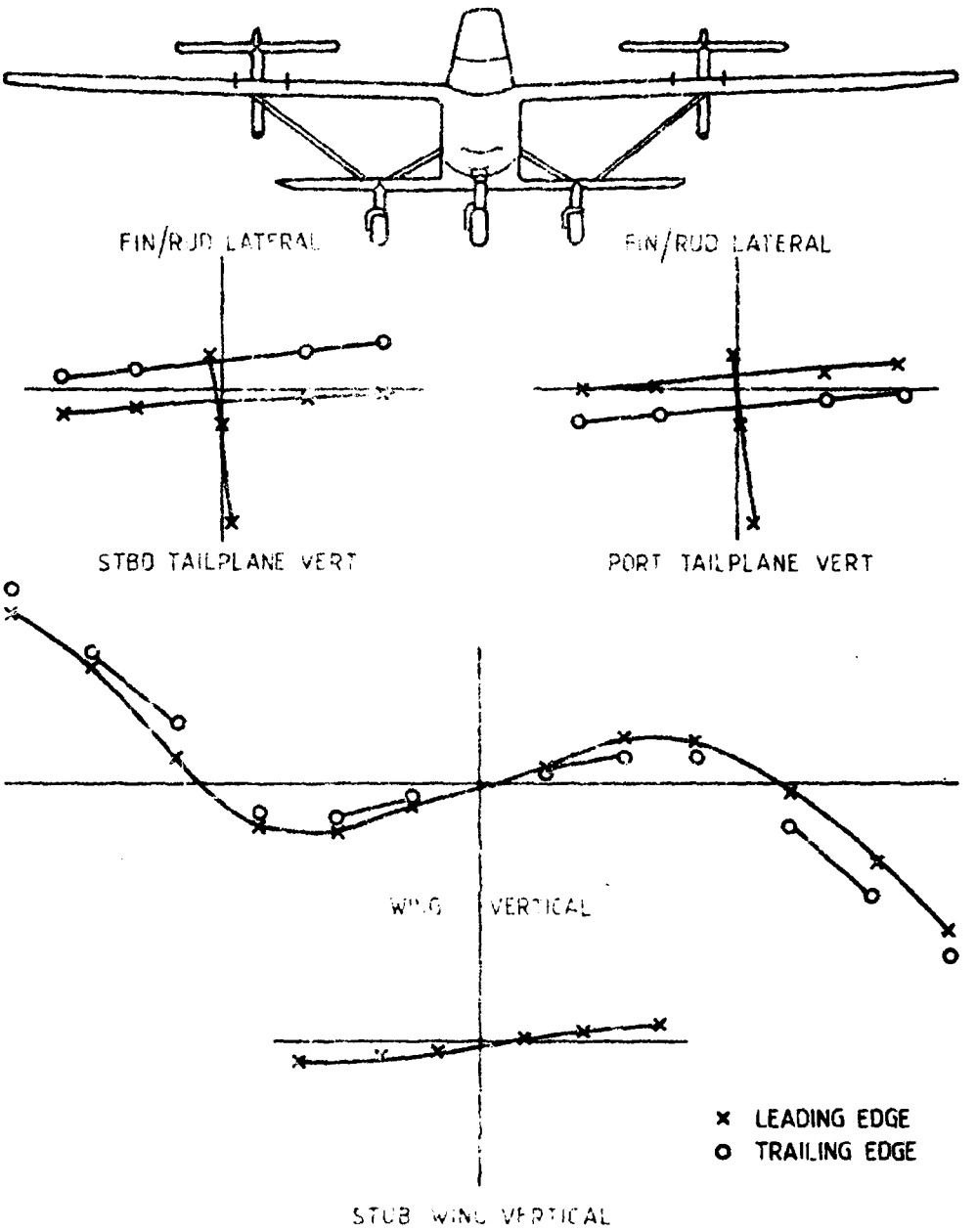

FIG.8(a) MODE AT 14.4 Hz

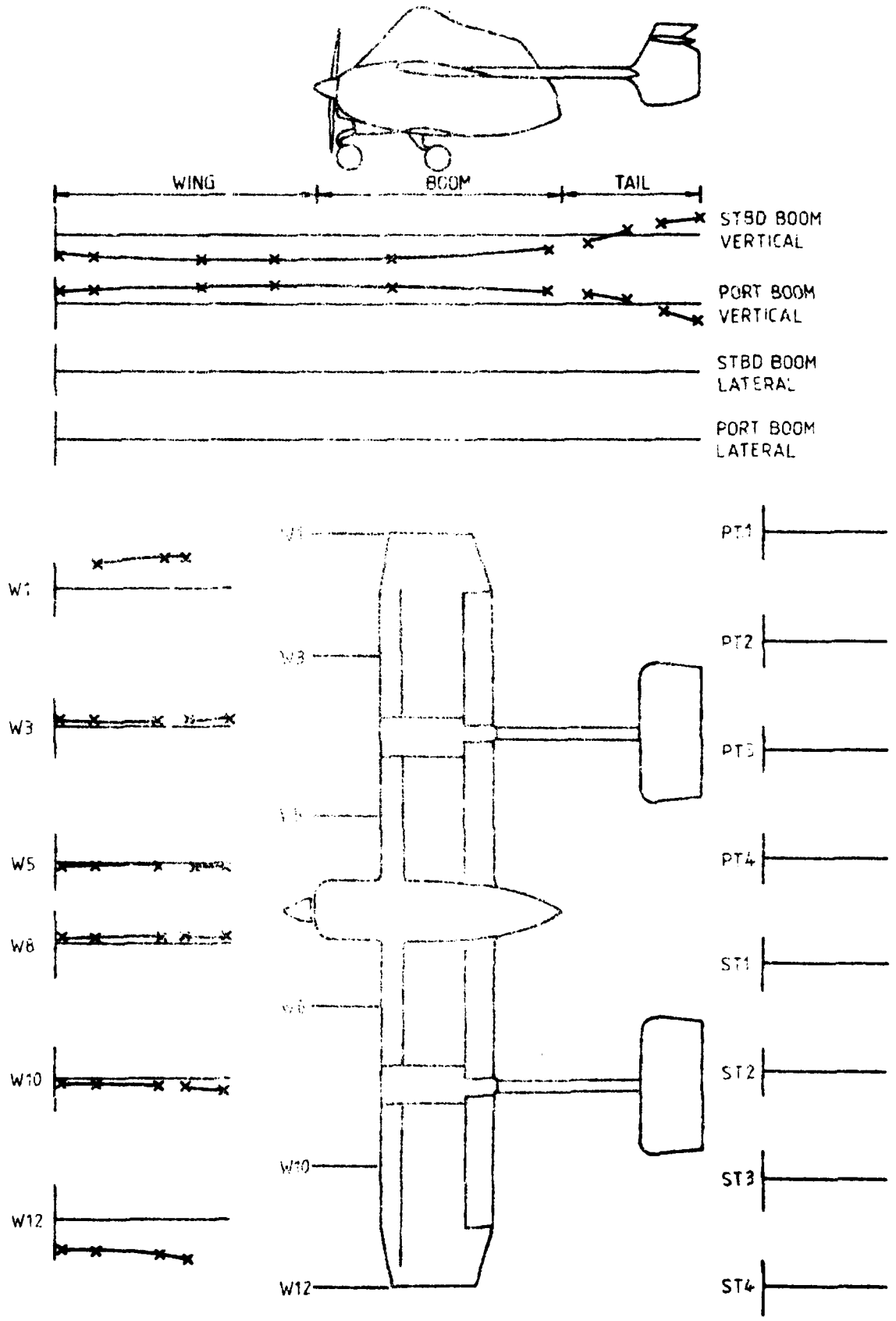

FIG.8(b) MODE AT 14.4 Hz

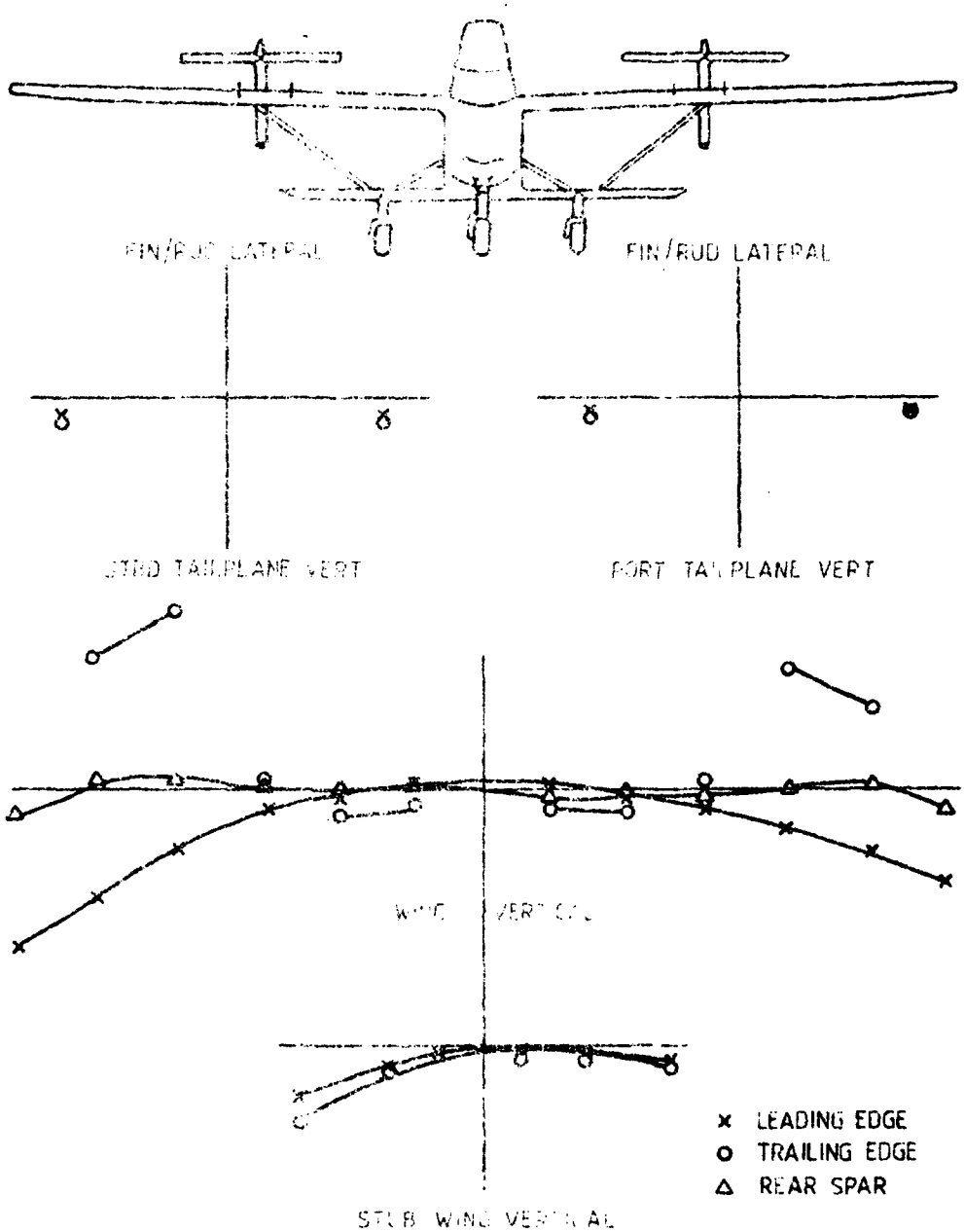

FIG.9(a) MODE AT 35.6 Hz

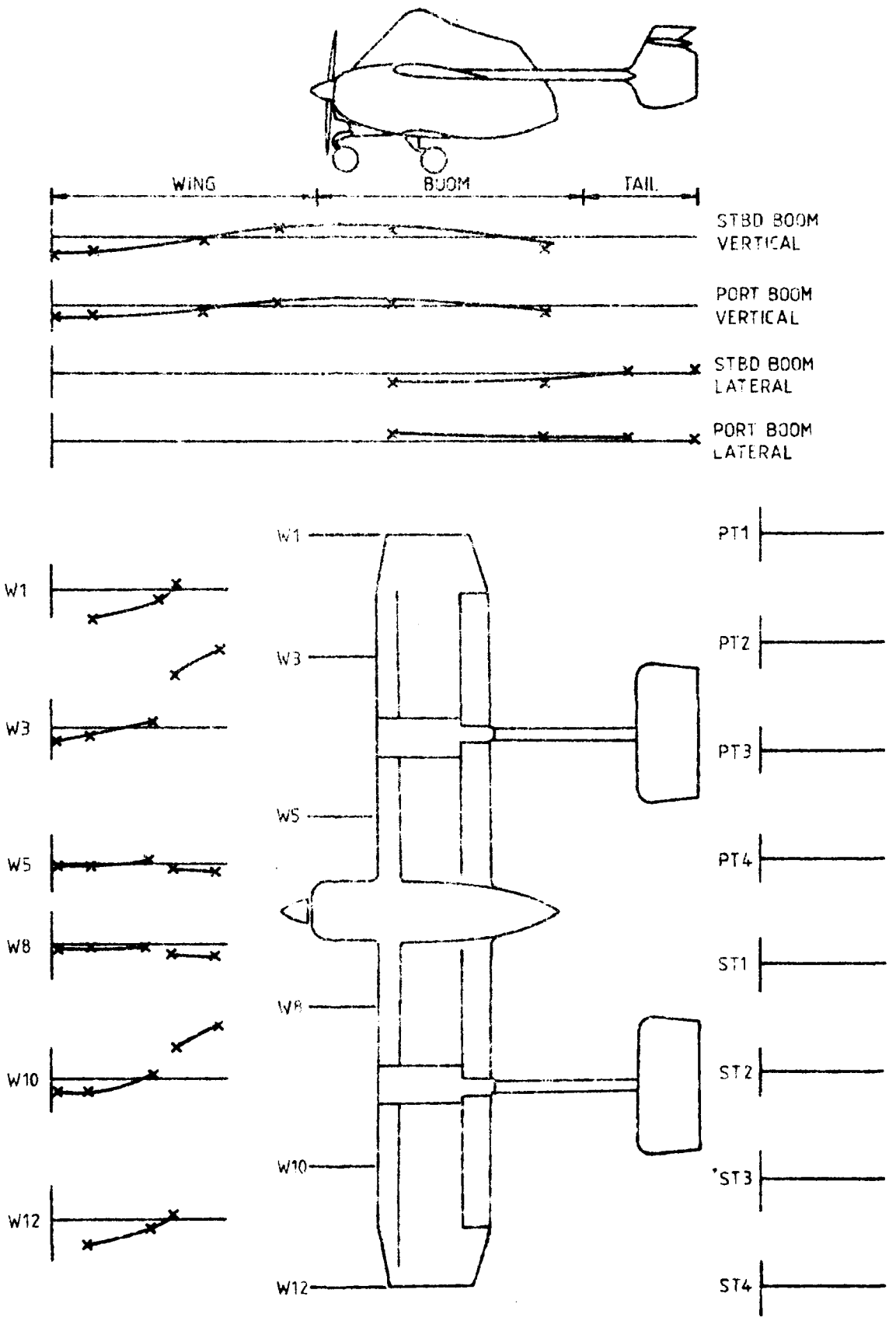

FIG.9(b) MODE AT 35.6 Hz

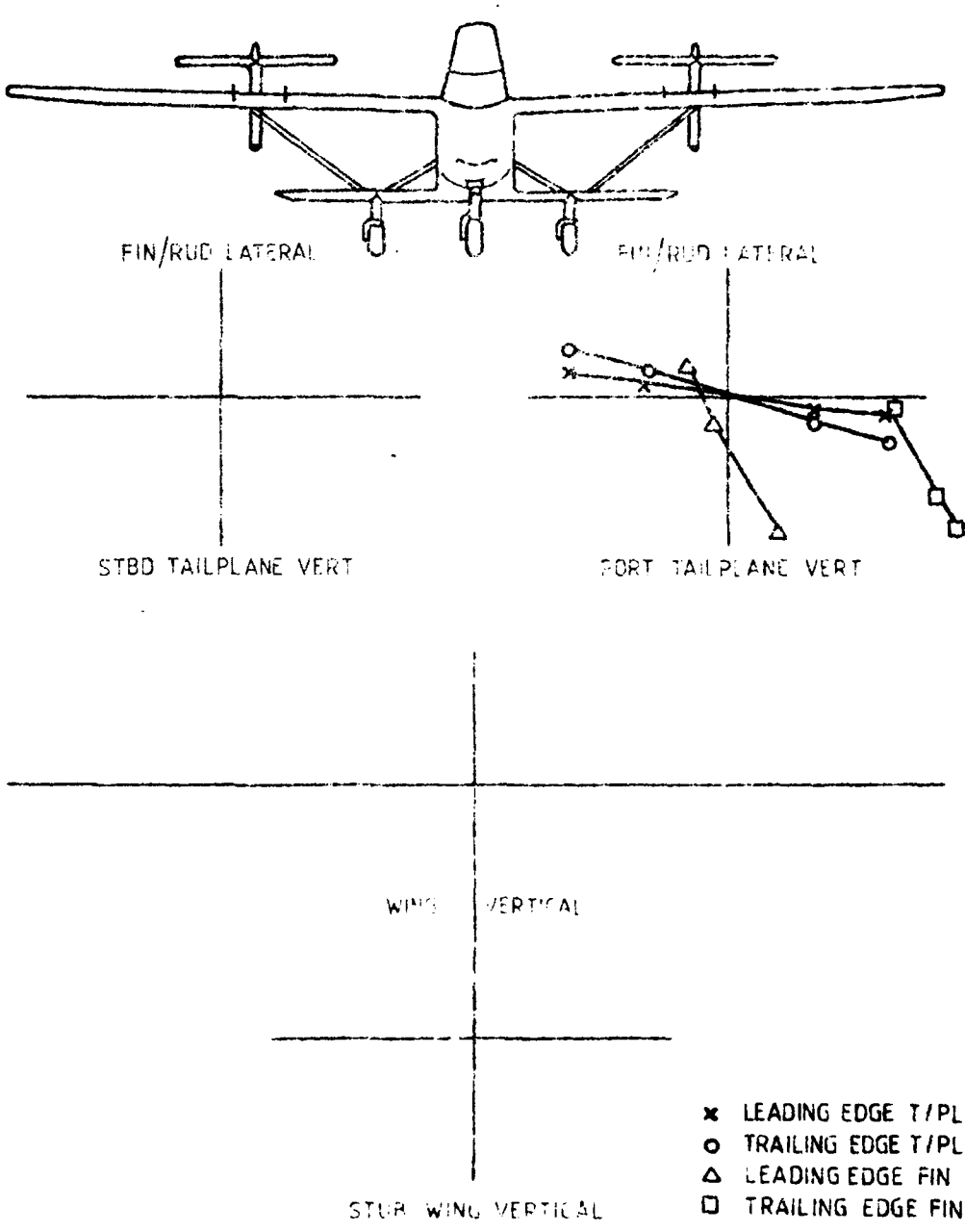

FIG.10(a) MODE AT 38 Hz

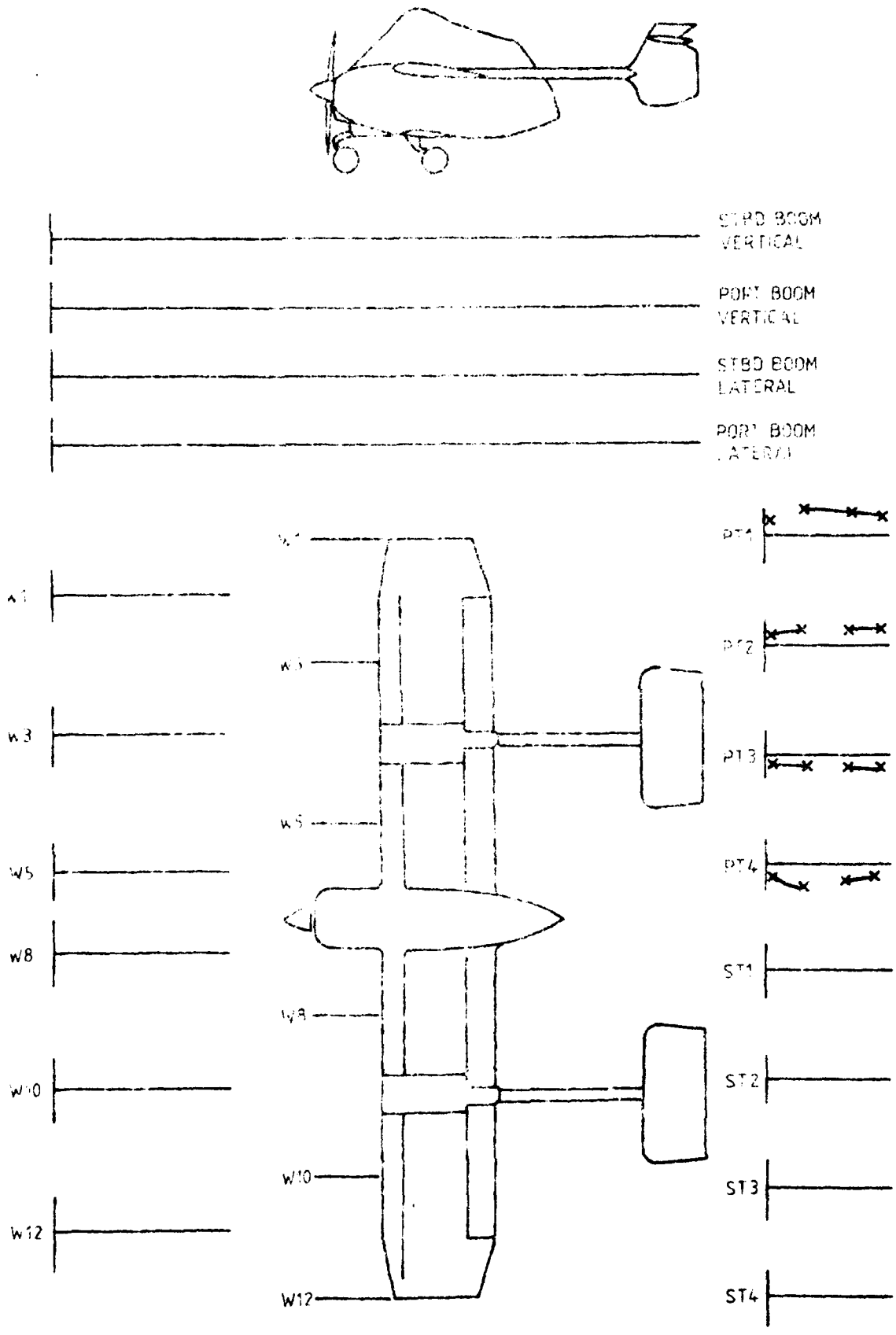

FIG. 10(c) MODE AT 38 Hz

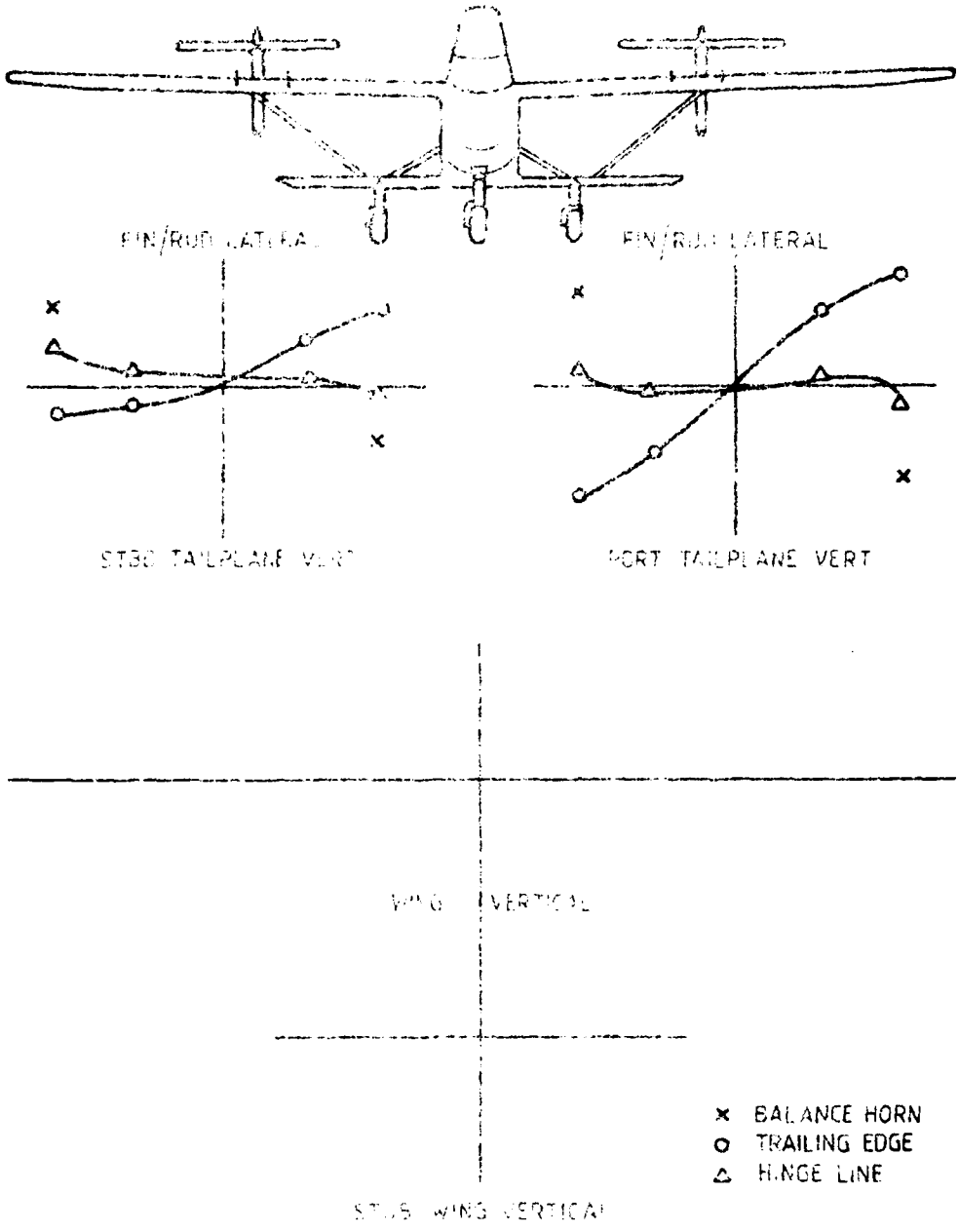

FIG.11(a) AGILE AT 30.4 KG

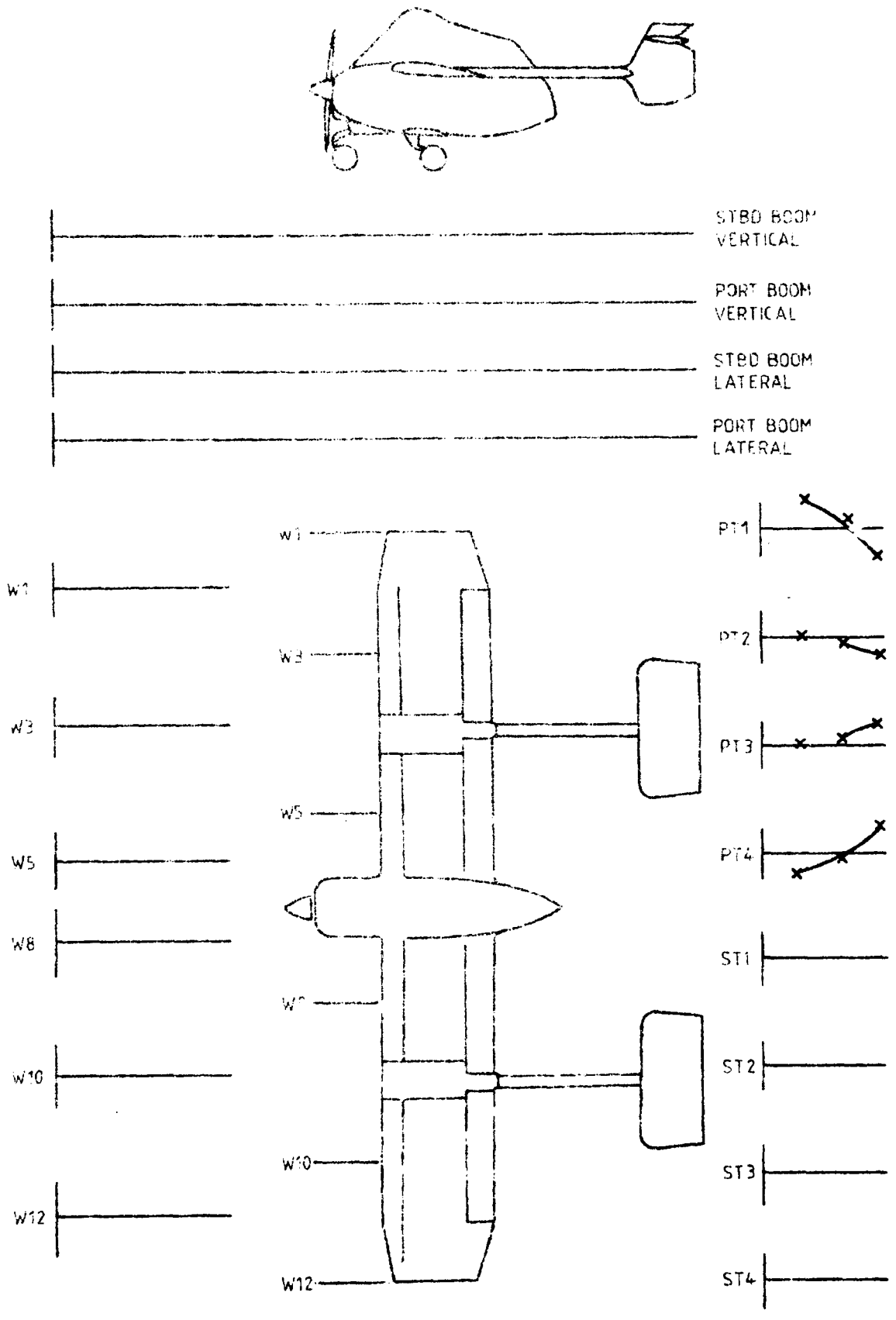

FIG.11(b) MODE AT [illegible]

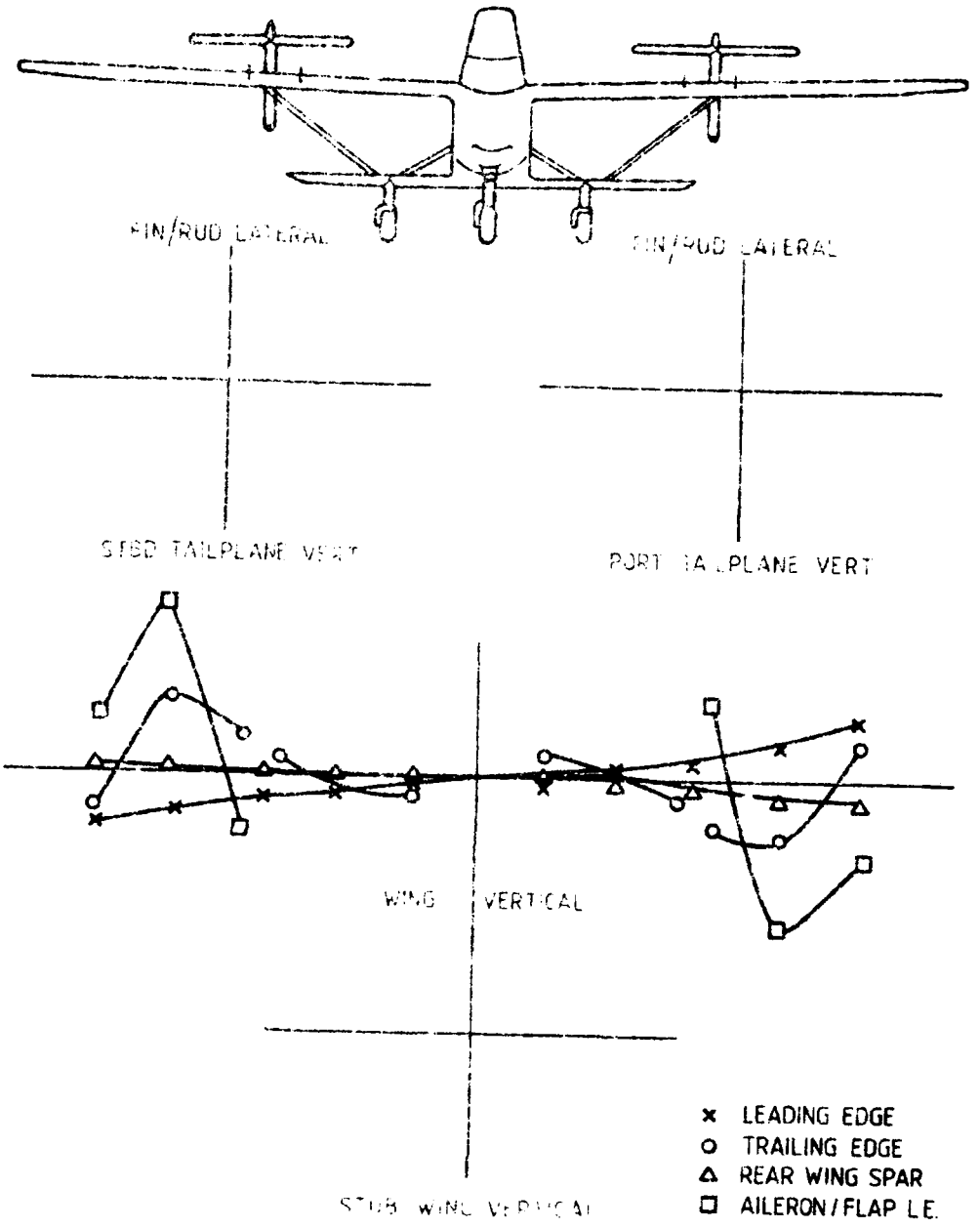

FIG.1.2(a) MODE A2 39.4 Hz

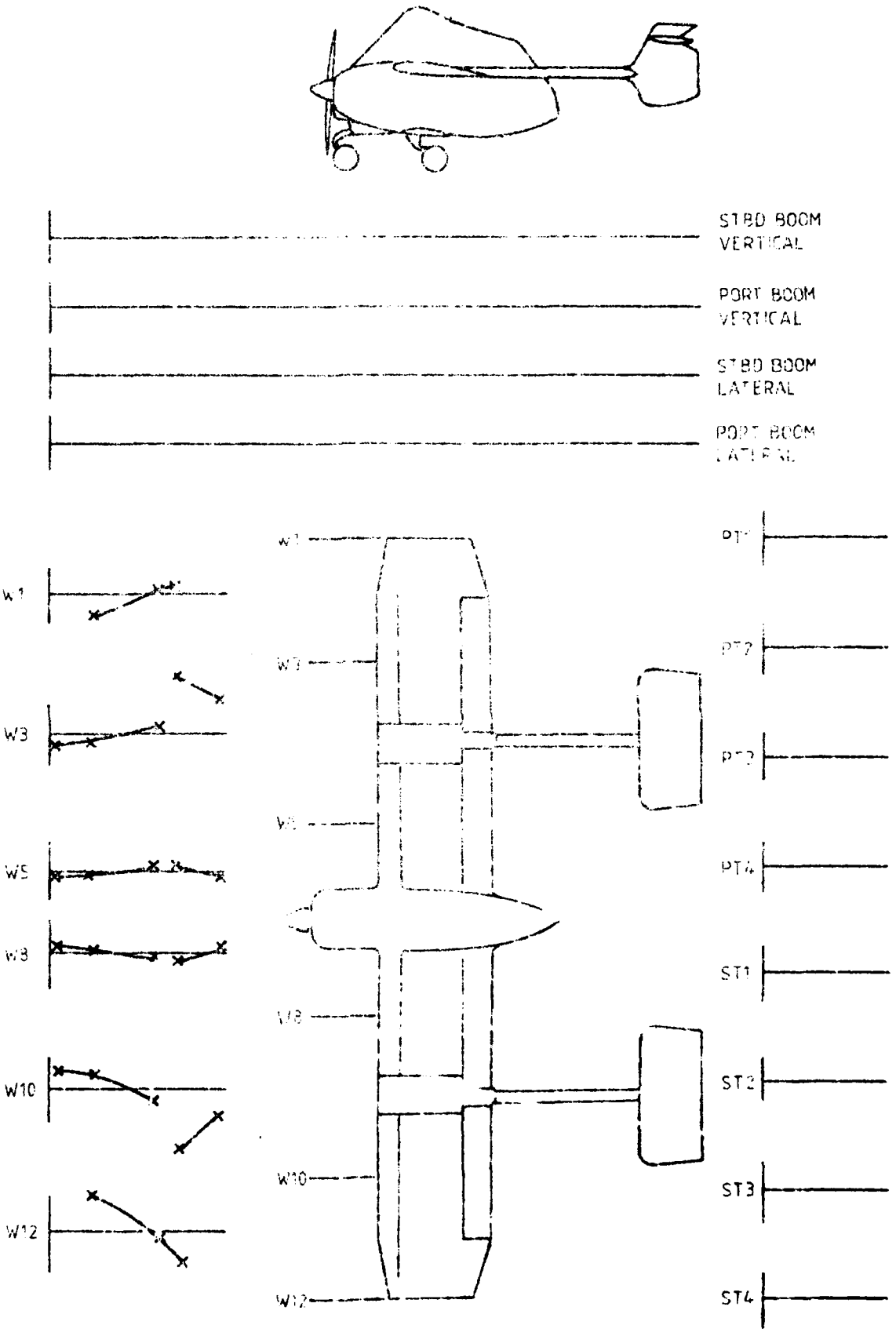

FIG. 1 (a) MODEL IN 16-A SR

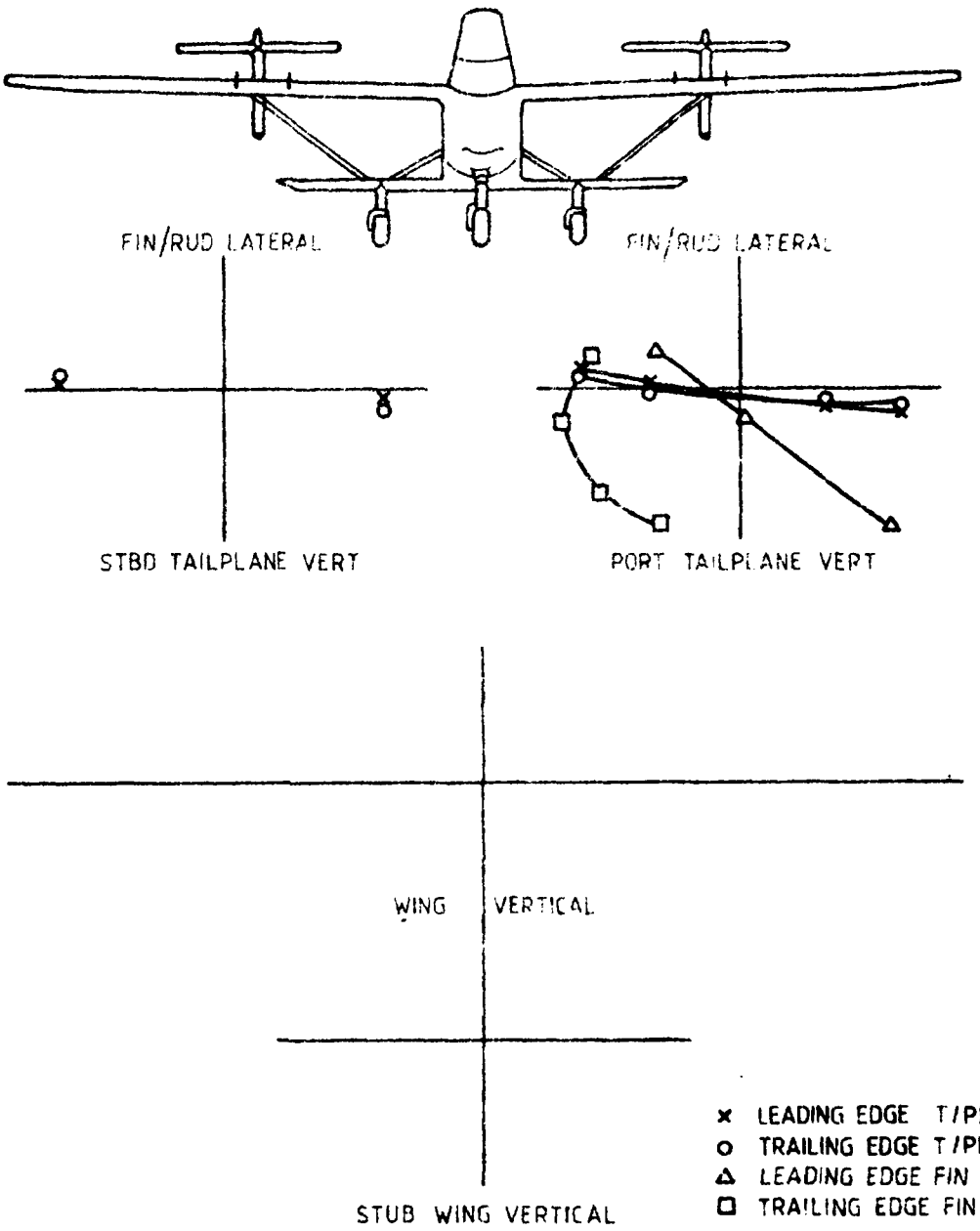

FIG.13(a) MODE AT 43.2 Hz

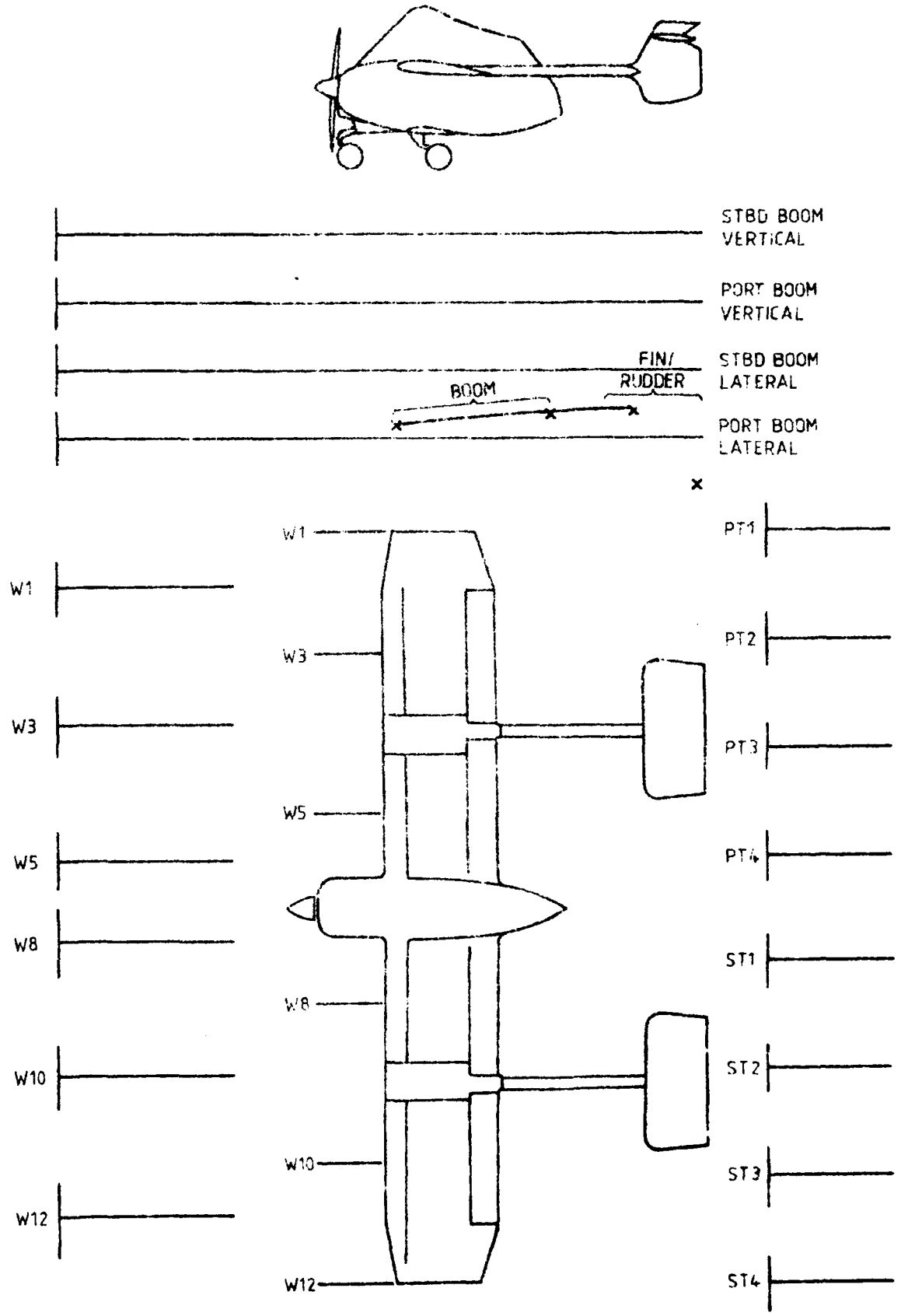

FIG.13(b) MODE AT 43.2 Hz

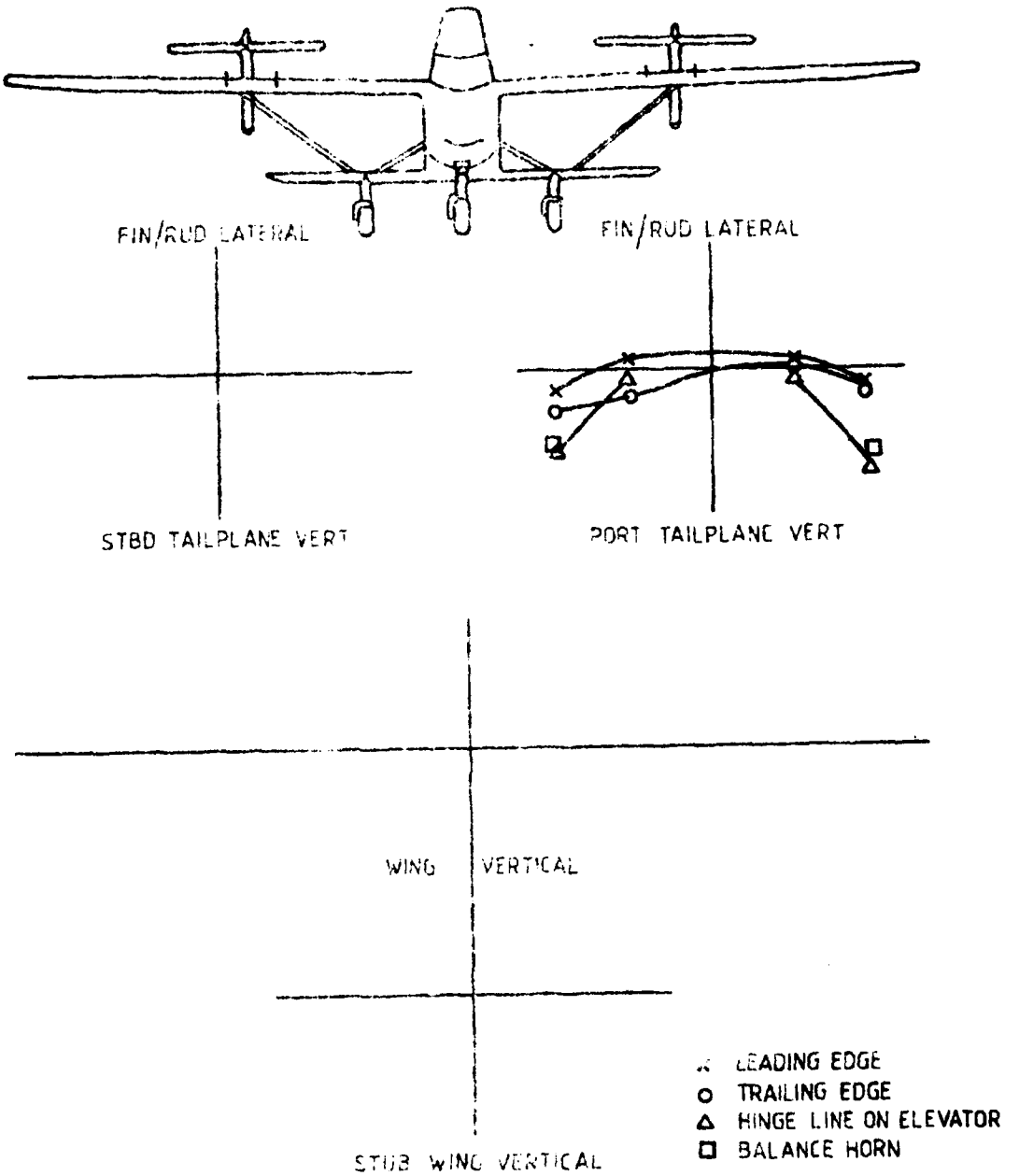

FIG.14(a) MODE AT 46.5 Hz

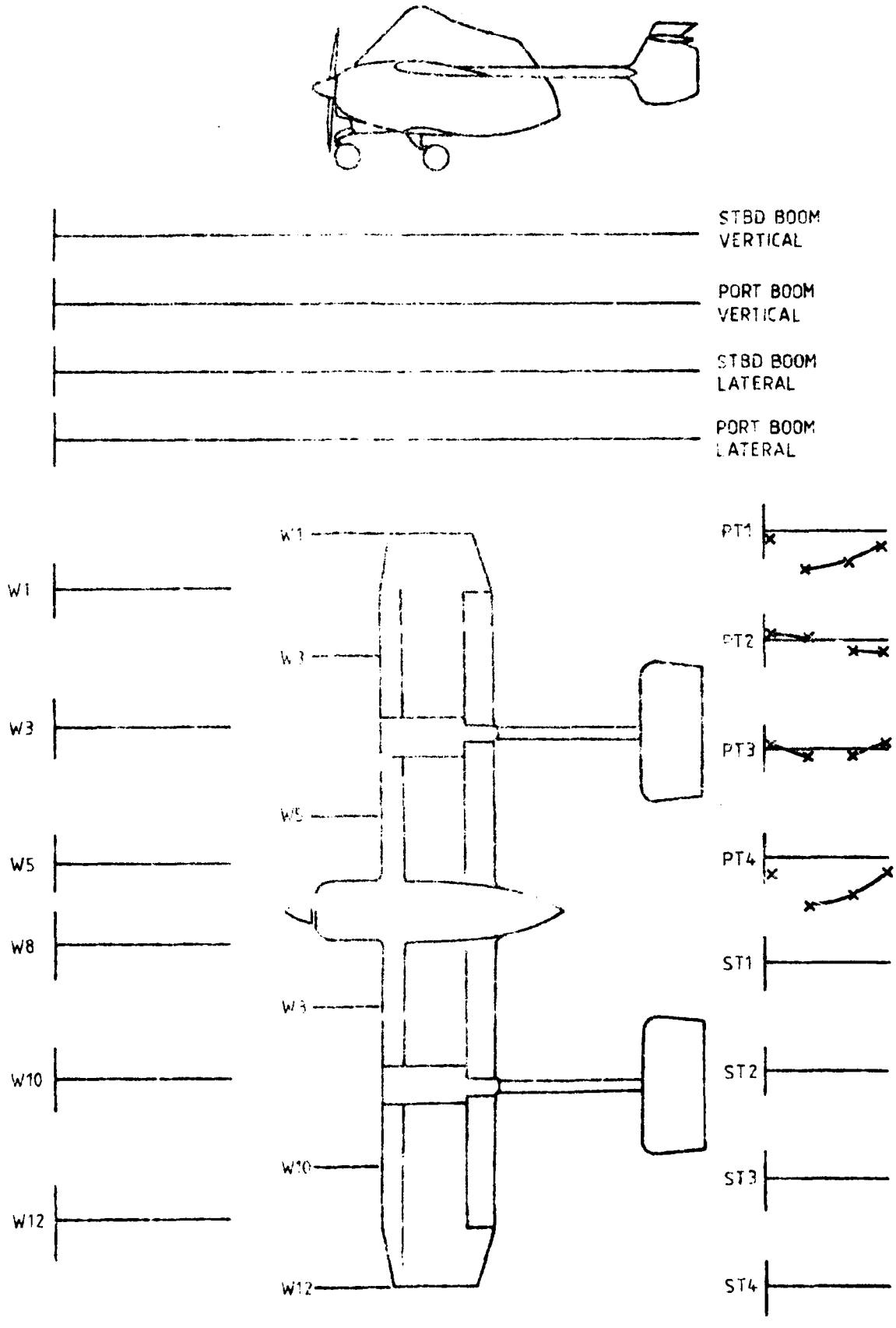

FIG. 14(c) MODE AT 46.5 Hz

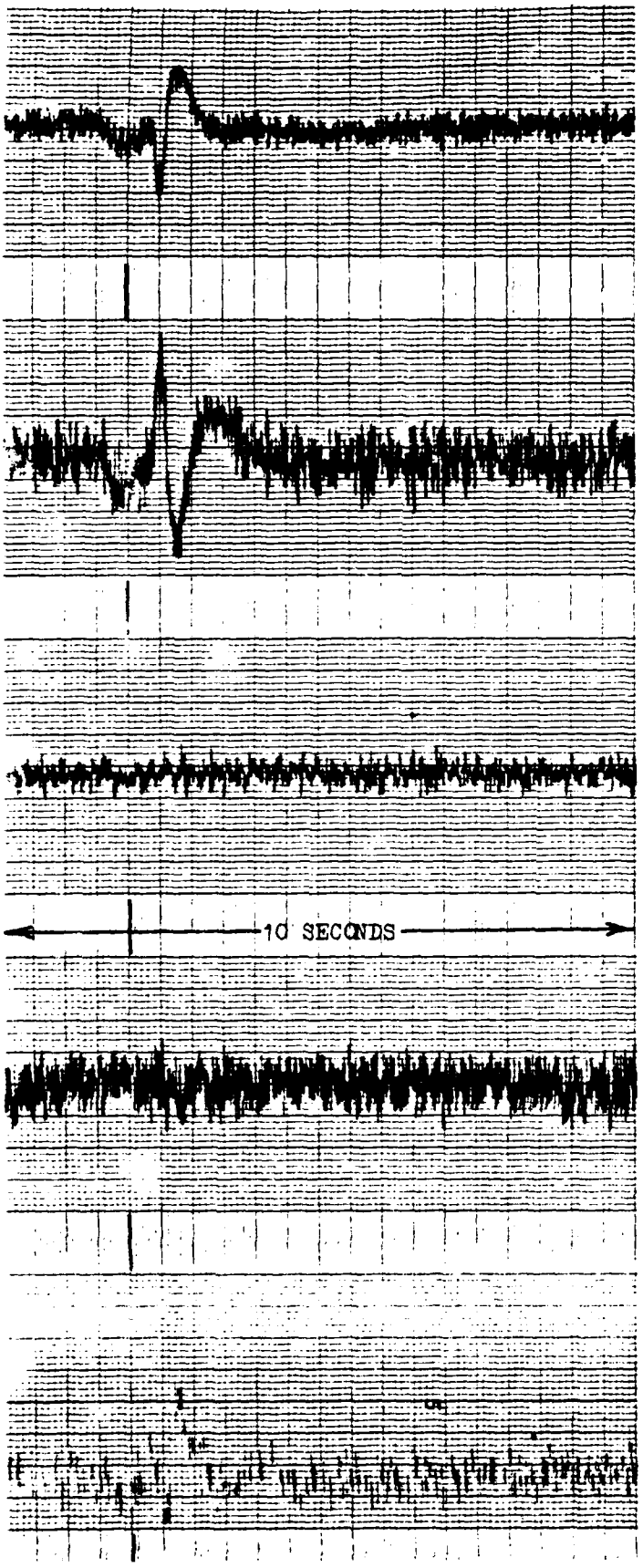

Port wing
Front spar
0.1g/cm

Starboard wing
Front spar
0.1g/cm

Port fin
top
0.1g/cm

Port rudder
top
0.2g/cm

Port wing
Rear spar
0.1g/cm

FIG.15(a) TEST POINT 2 - 117 KNOTS I.A.S.

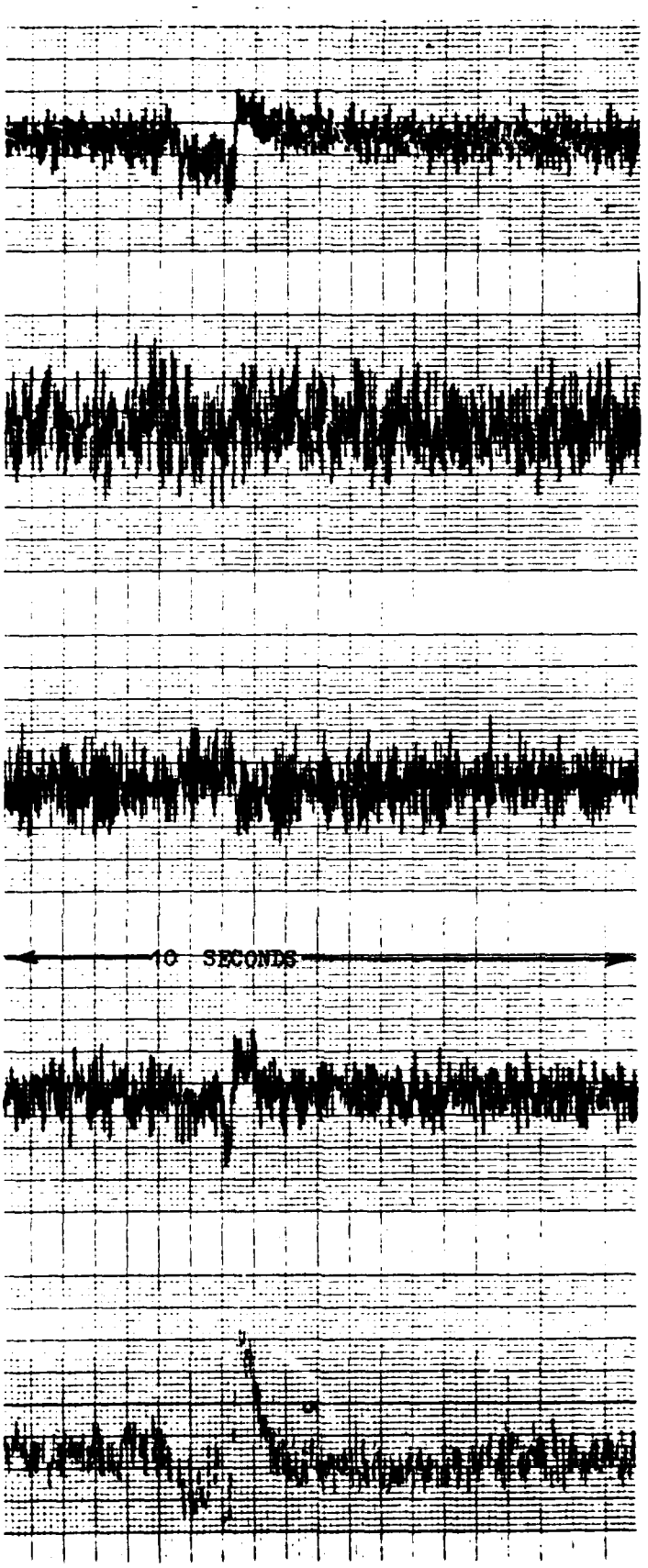

Port boom
vertical
0.2g/cm

Port tailplane
0.1g/cm

Port elevator
0.1g/cm

Port aileron
0.1/g

Port wing
Front spar
0.1g/cm

FIG.15(b) TEST POINT 2 - 117 KNOTS I.A.S.

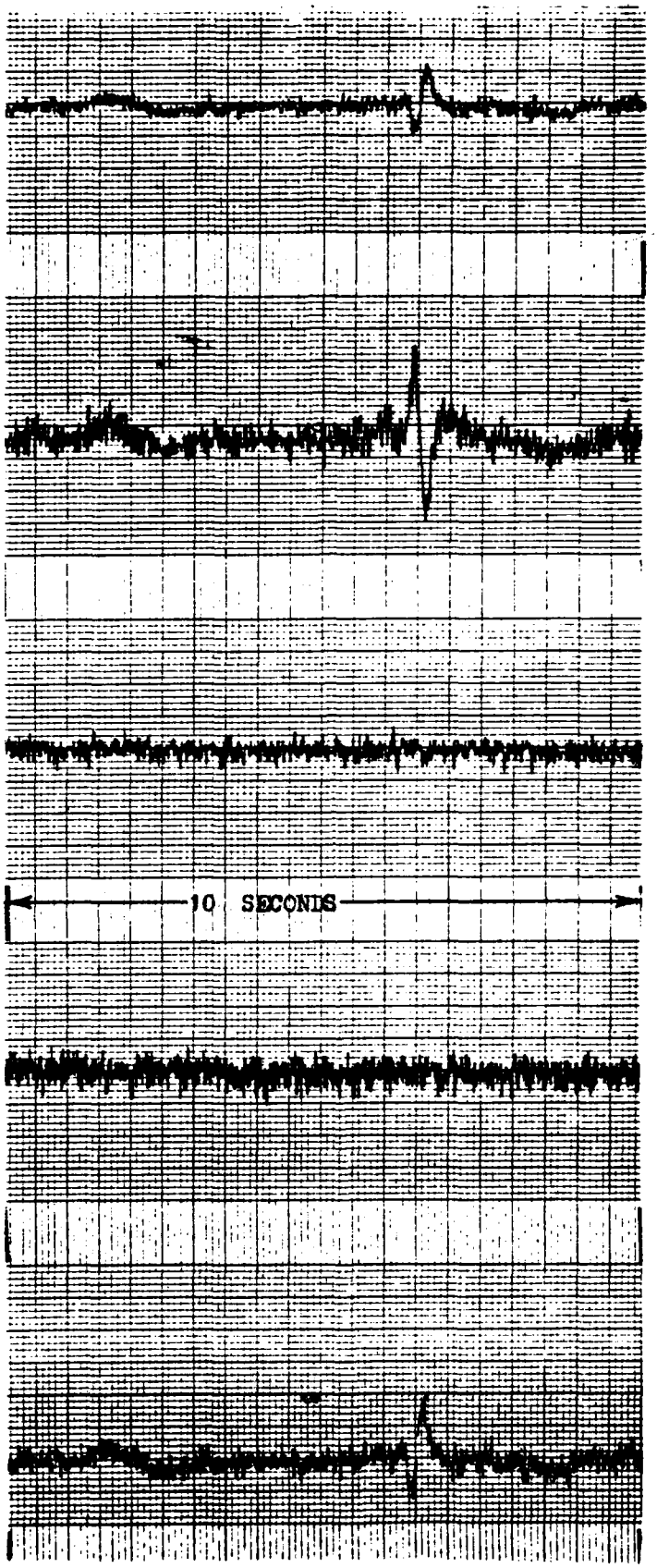

Port wing
Front spar
1g/cm

Starboard wing
Front spar
1g/cm

Port fin
top
1g/cm

Port rudder
top
2g/cm

Port wing
Rear spar
1g/cm

FIG.15(c) TEST POINT 12 - 175 KNOTS I.A.S.

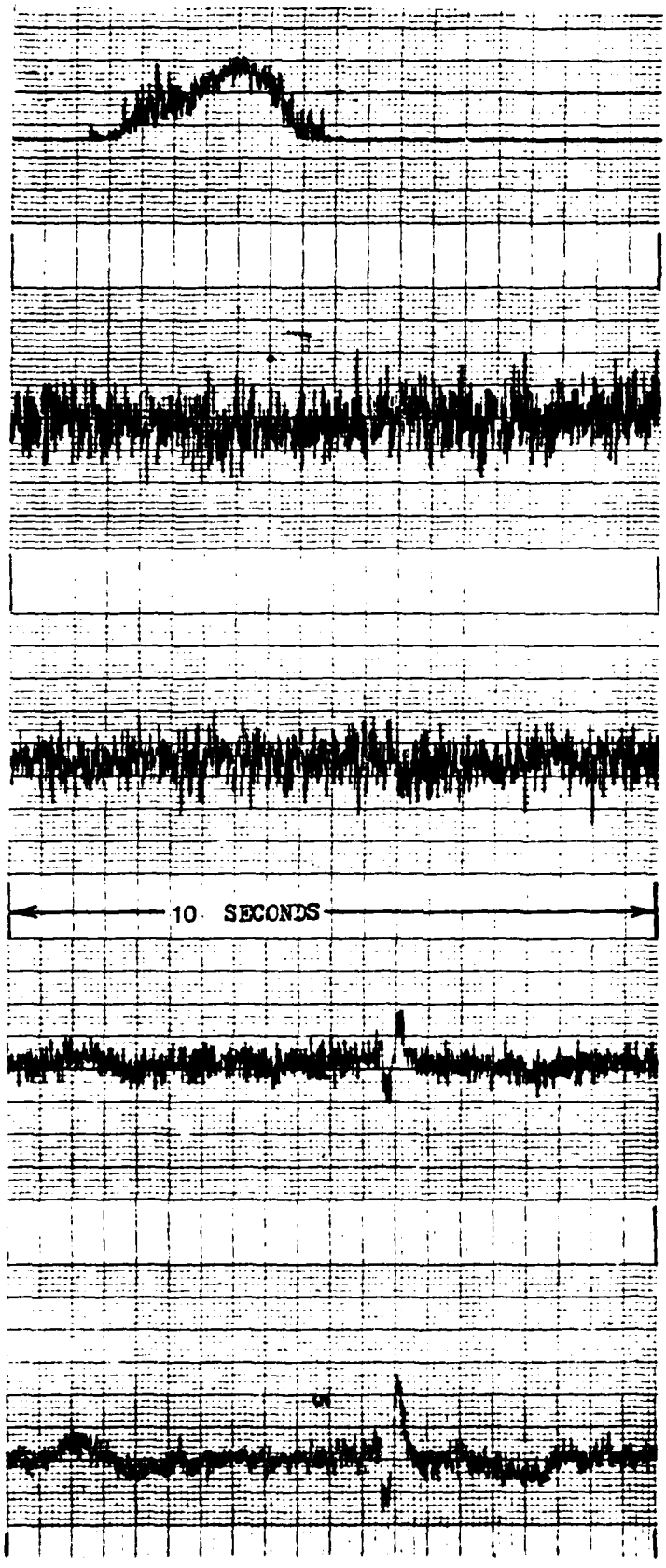

Port boom
vertical
2g/cm

Port tailplane
1g/cm

Port elevator
1g/cm

Port aileron
1g/cm

Port wing
Front spar
1g/cm

FIG.15(d) TEST POINT 12 - 175 KNOTS I.A.S.

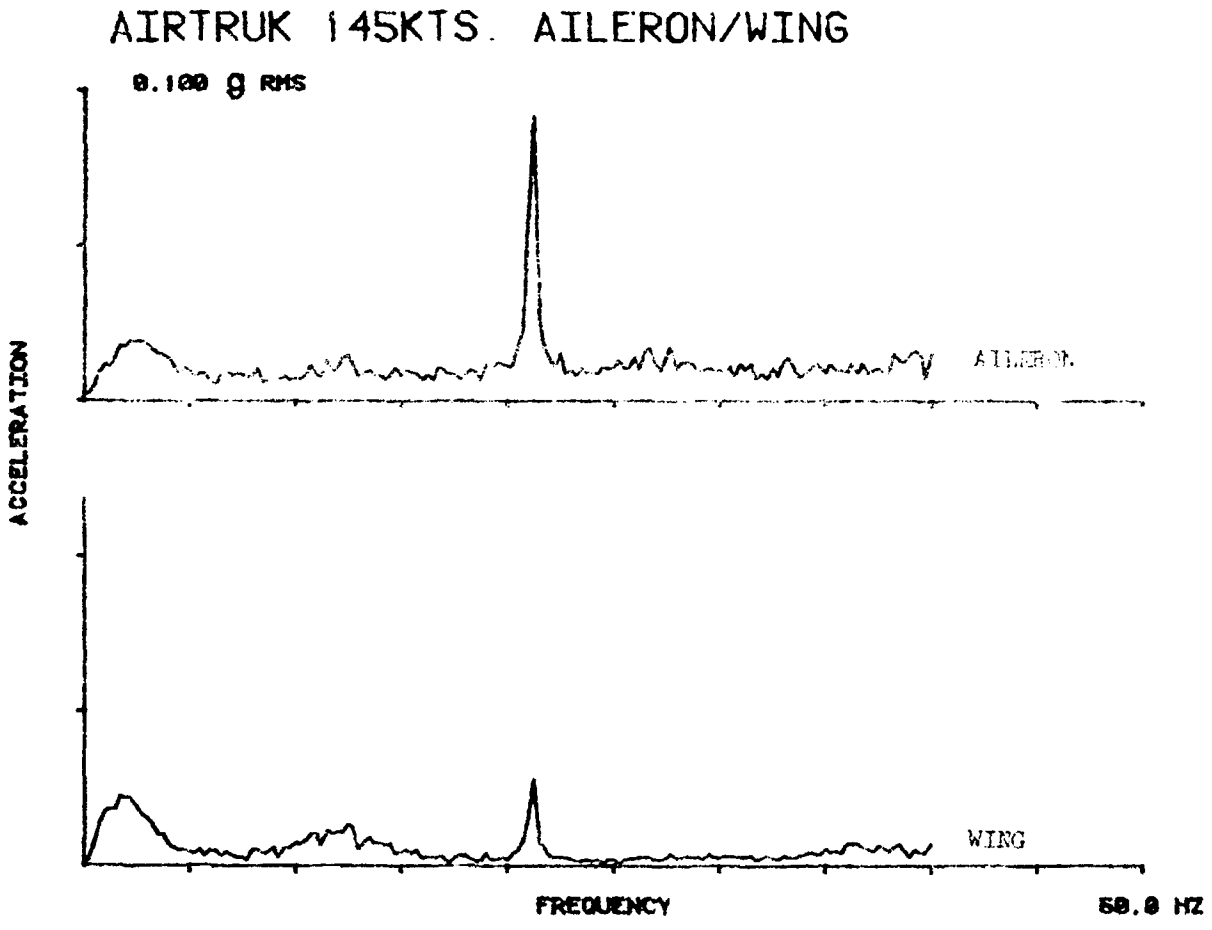

FIG.16(a) FREQUENCY RESPONSE AT 145 KNOTS I.A.S.

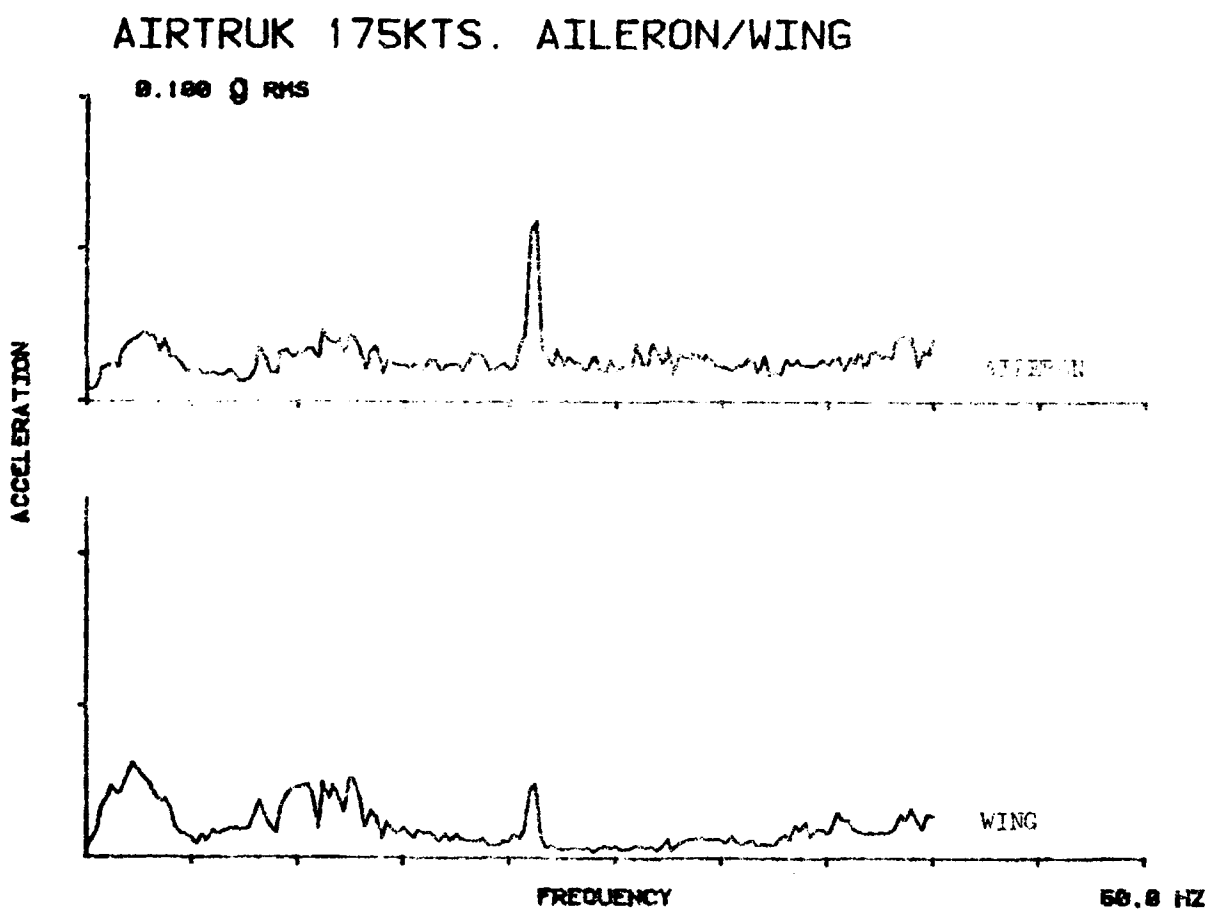

FIG.16(b) FREQUENCY RESPONSE AT 175 KNOTS I.A.S.

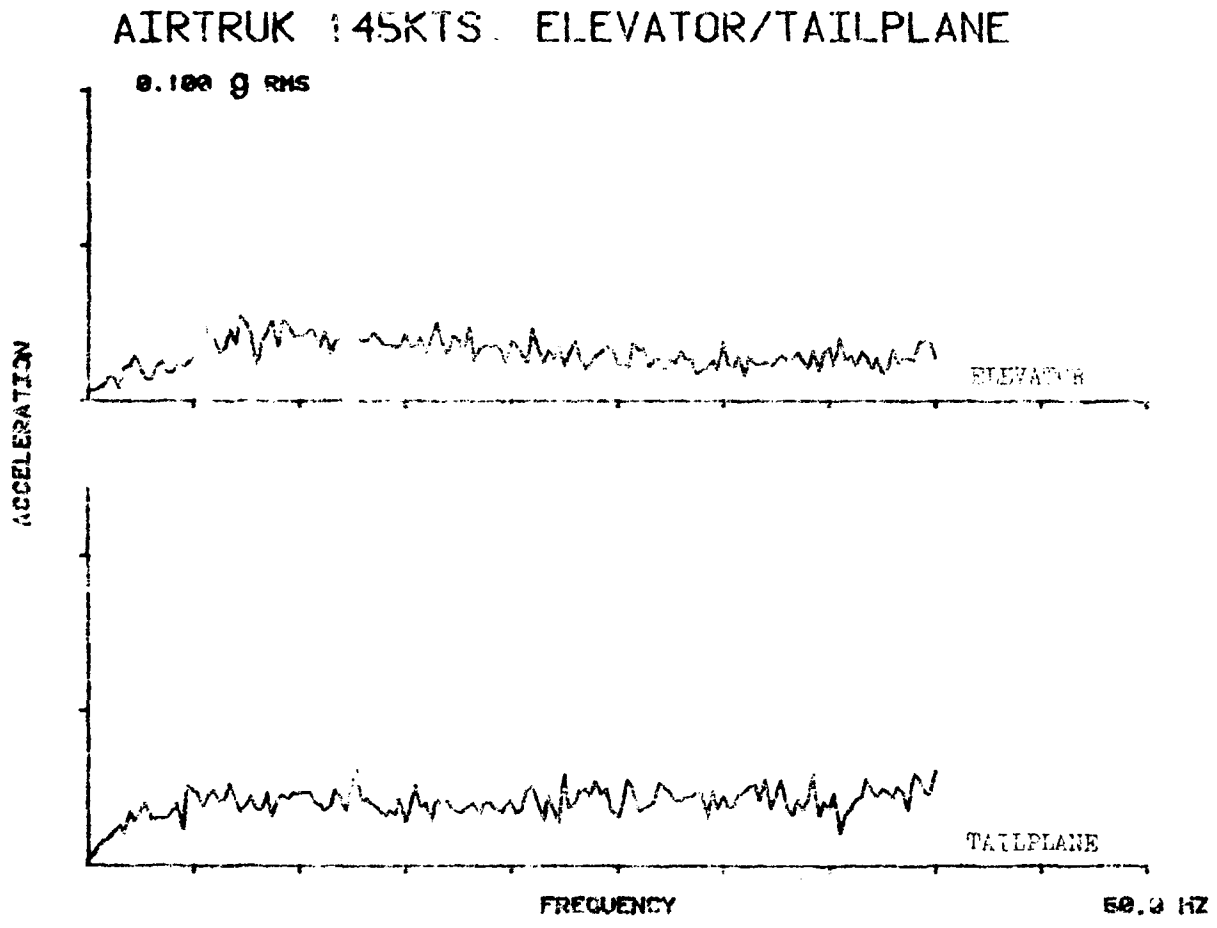

FIG.17(a) FREQUENCY RESPONSE AT 145 KNOTS T.A.S.

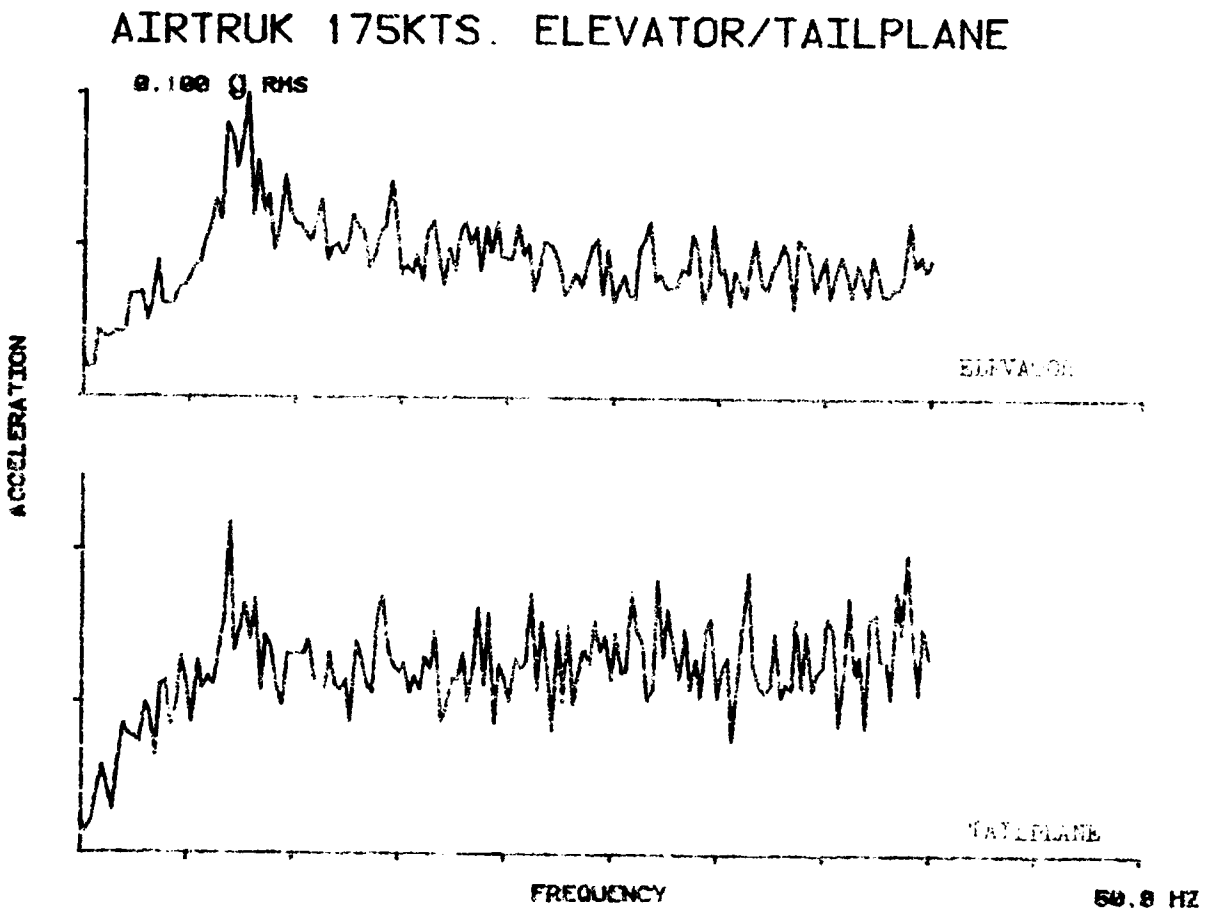

FIG.17(i) FREQUENCY RESPONSE AT 175 KNOTS I.A.S.

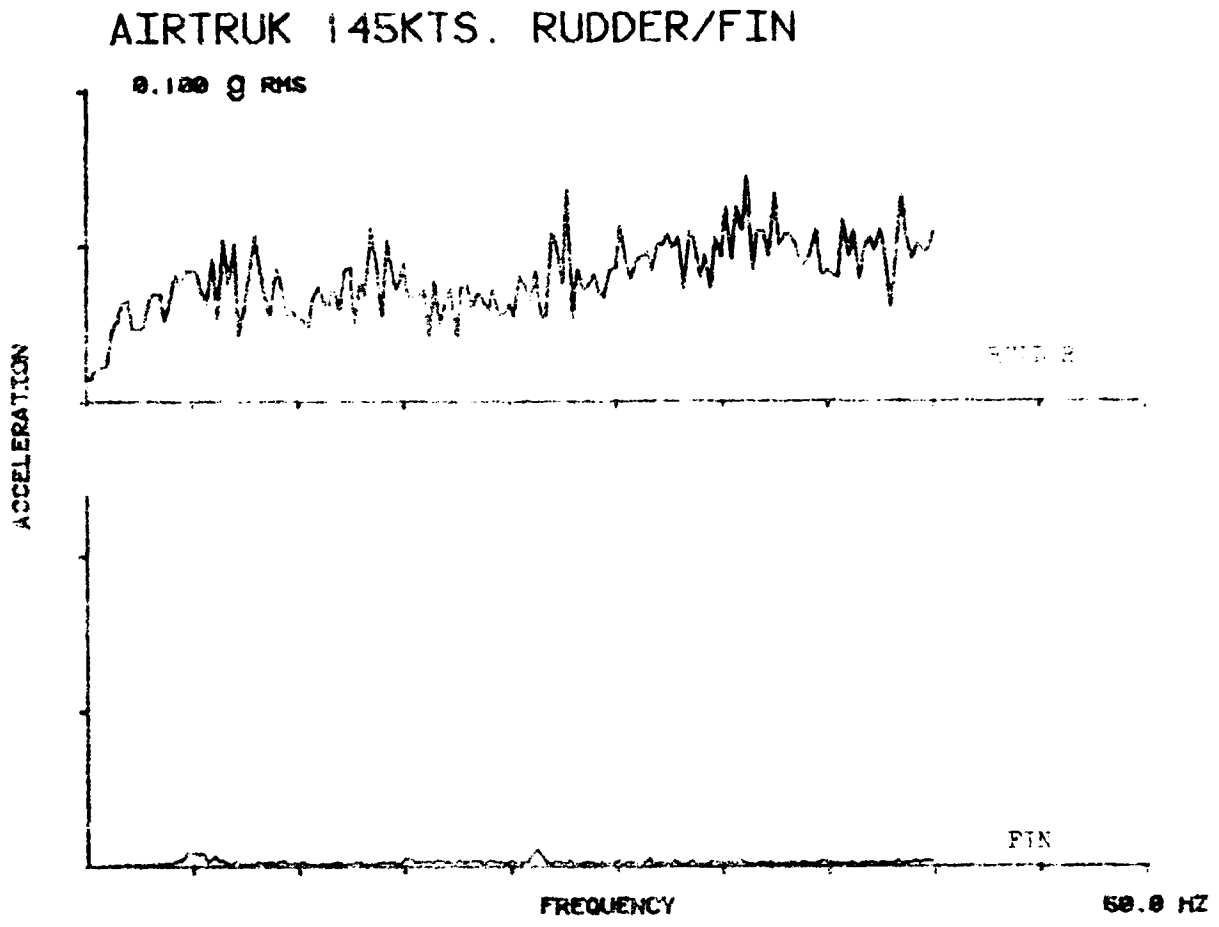

FIG.13(a) FREQUENCY RESPONSE AT 145 KNOTS I.A.S.

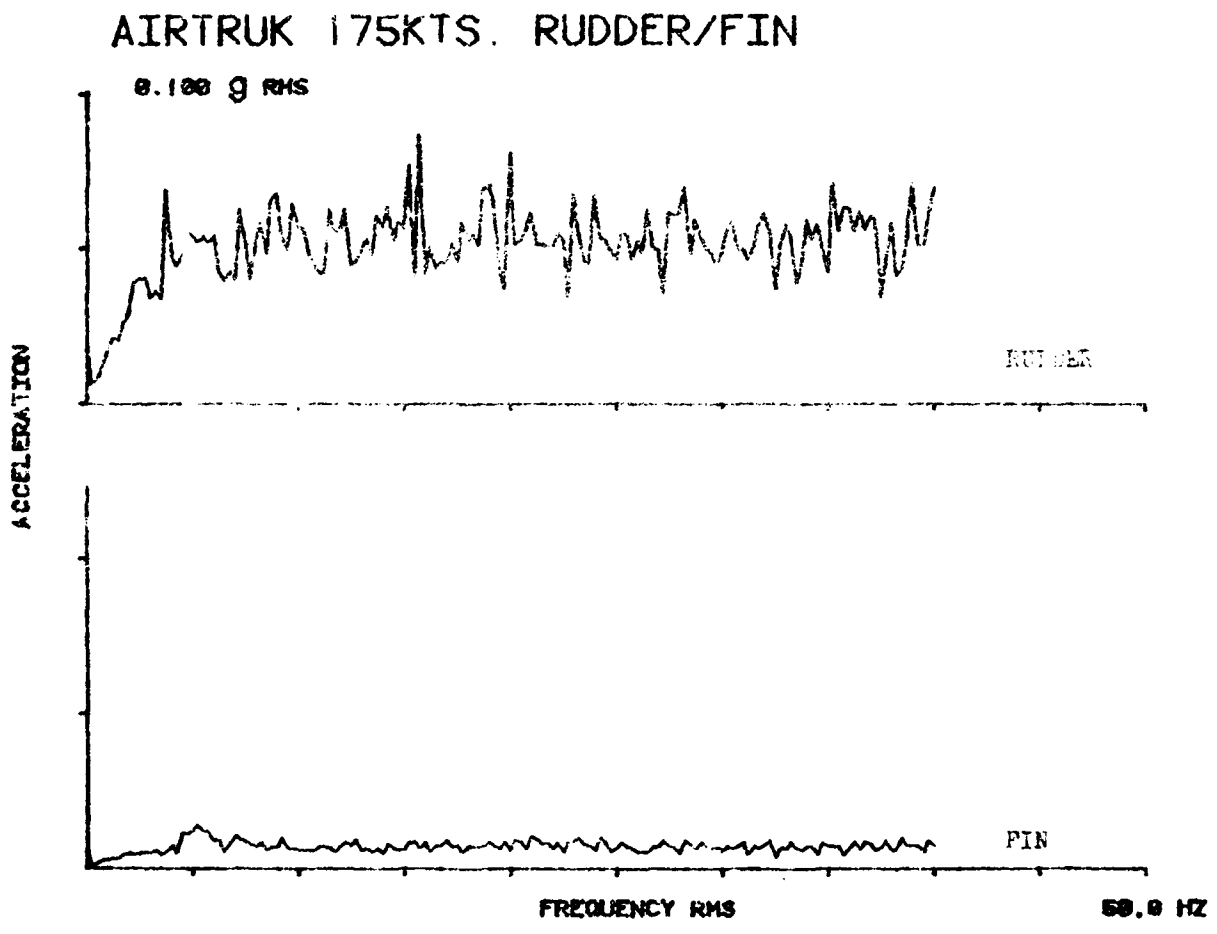

FIG.18(b) FREQUENCY RESPONSE AT 175 KNOTS I.A.S.

AIRTRUK AT 175 Knots .... LOW-PASS FILTER AT 10 Hz

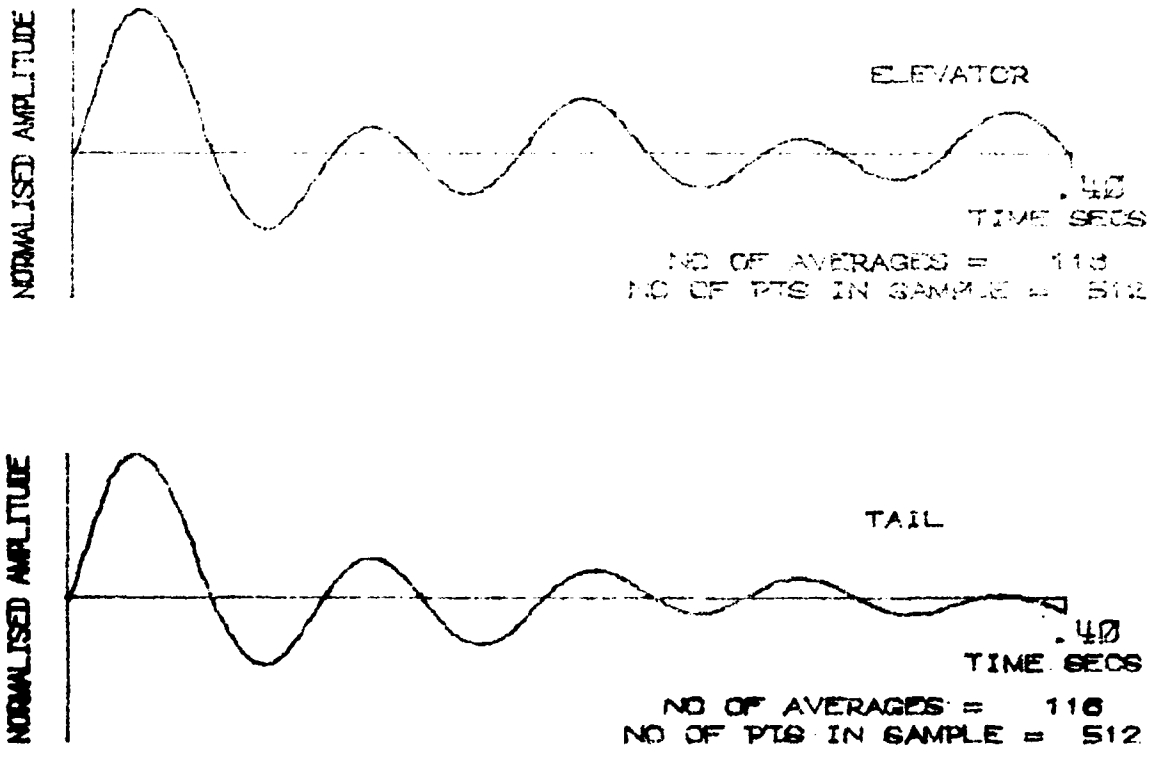

F.G.19(a) RANDOM DECREMENT SIGNATURE

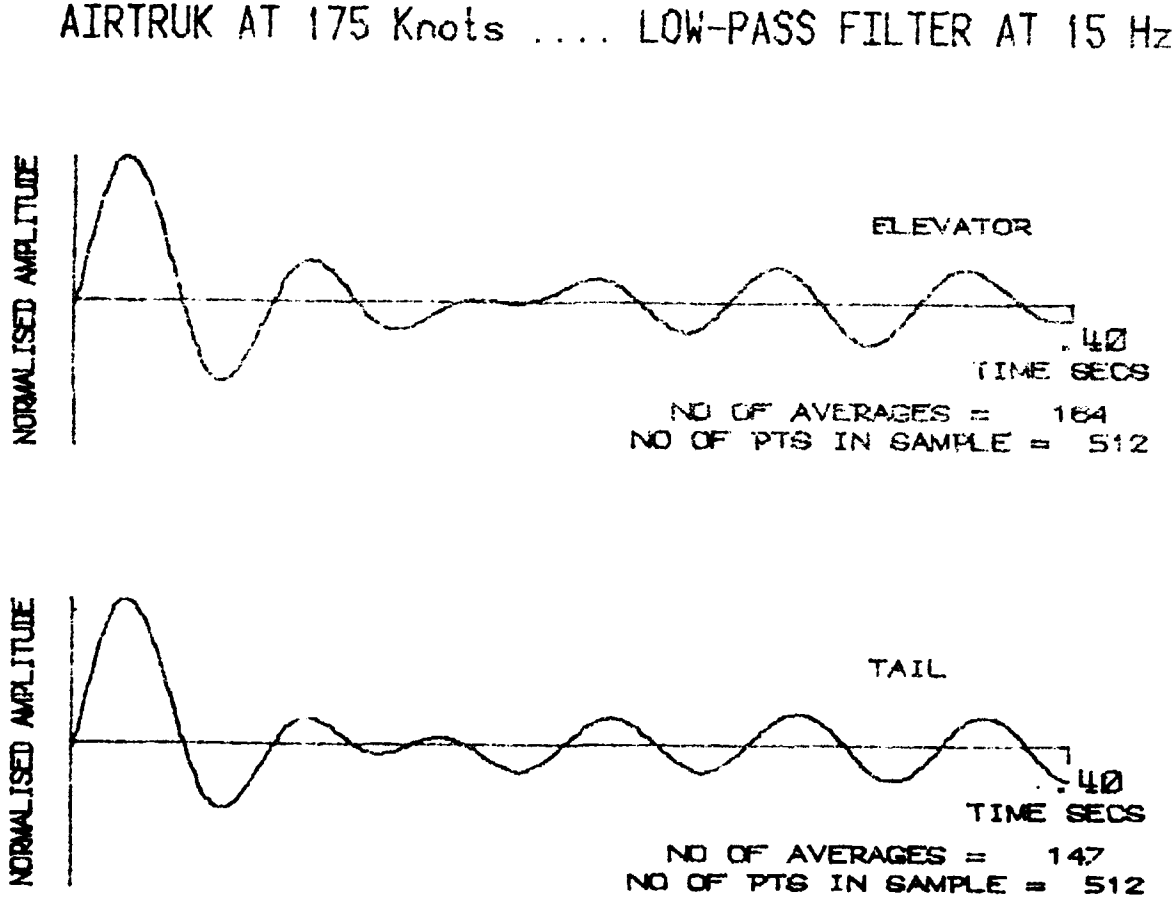

FIG.19(b) RANDOM DECREMENT SIGNATURE

AIRTRUK AT 175 Knots .... LOW-PASS FILTER AT 20 Hz

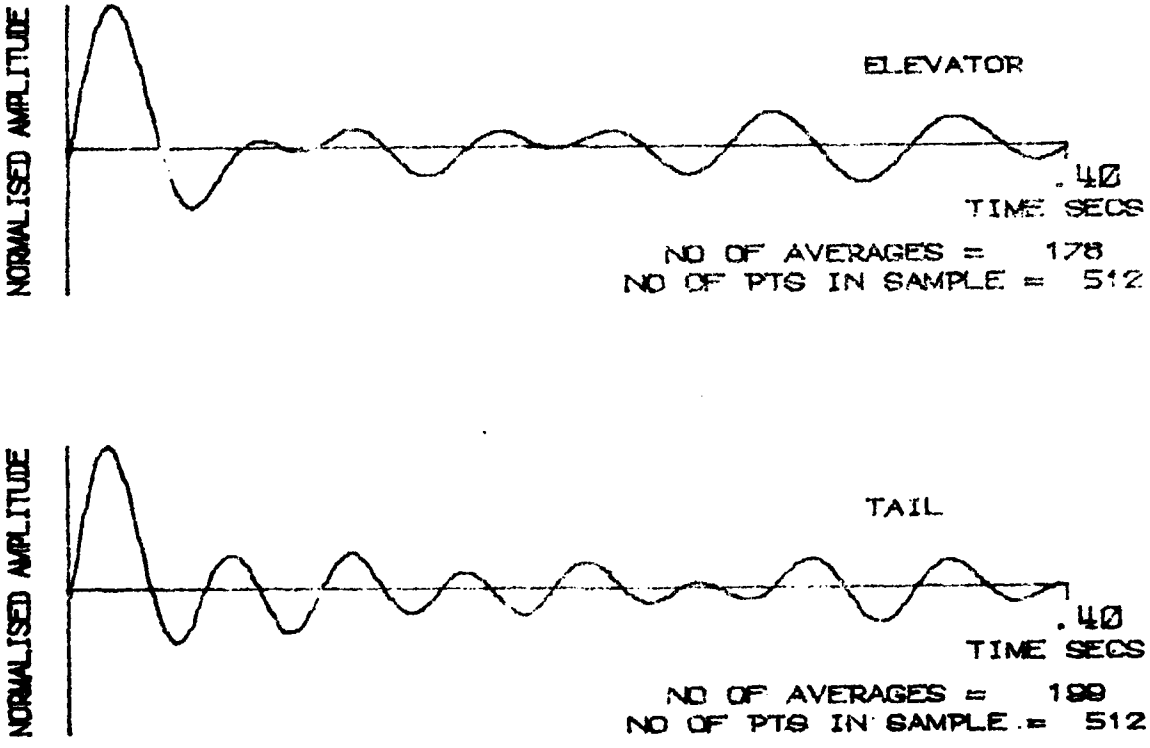

FIG.19(c) RANDOM DECREMENT SIGNATURE

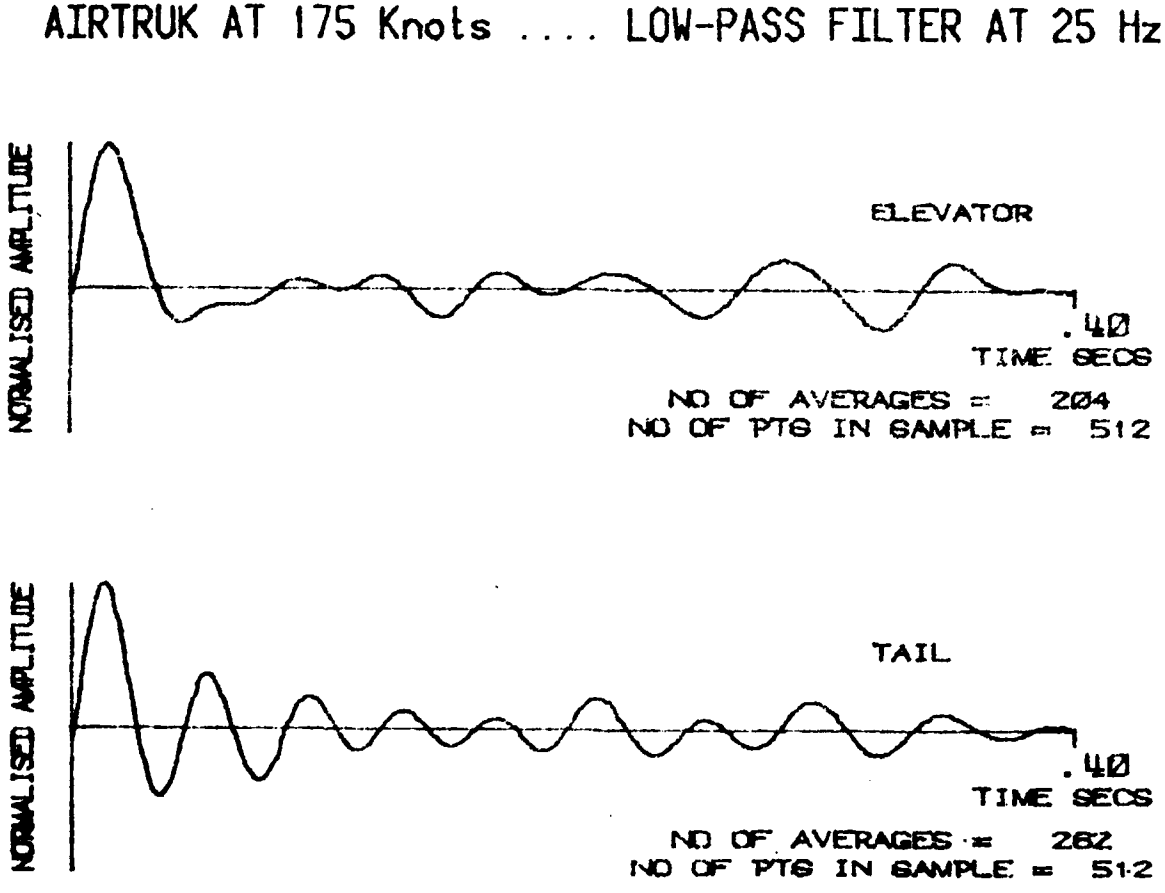

FIG.19(d) RANDOM DECREMENT SIGNATURE

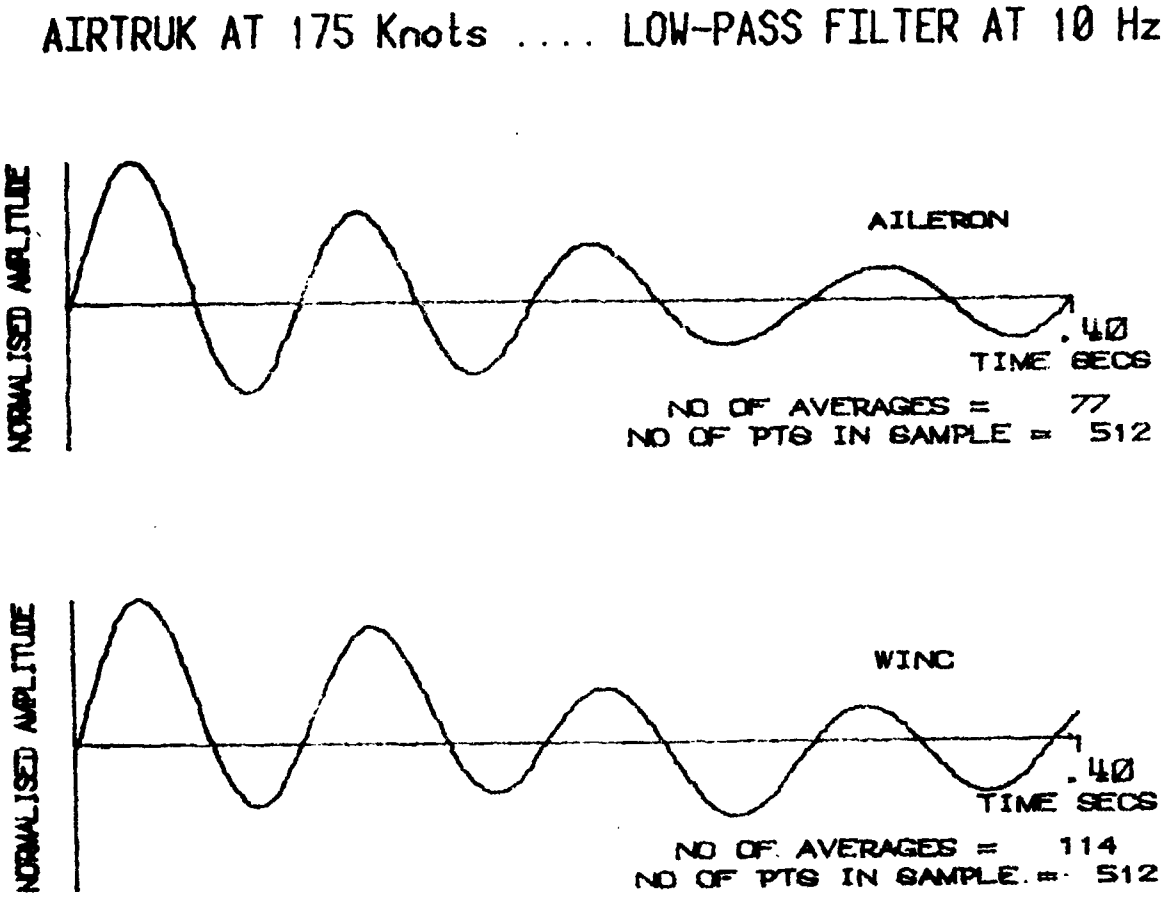

FIG.20(a) RANDOM DECREMENT SIGNATURE

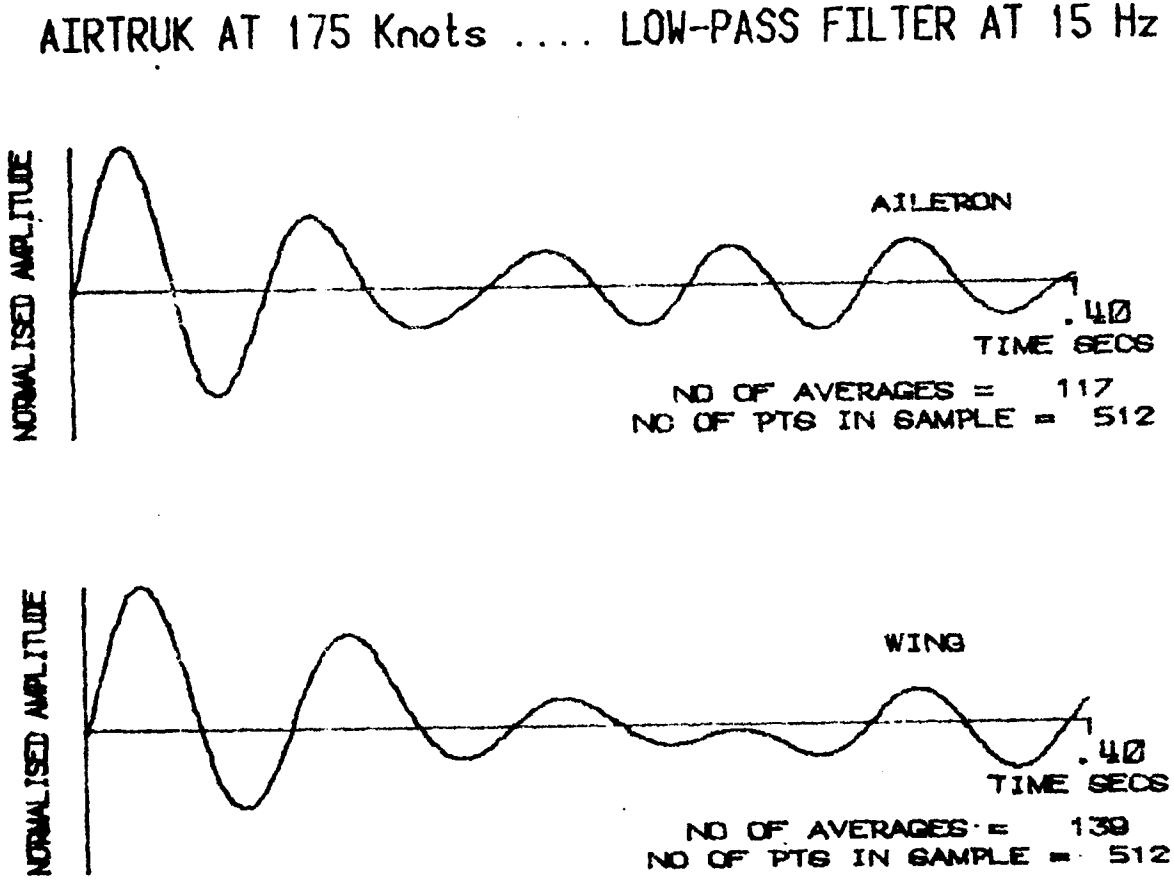

FIG.20(b) RANDOM DECREMENT SIGNATURE

AIRTRUK AT 175 Knots .... LOW-PASS FILTER AT 20 Hz

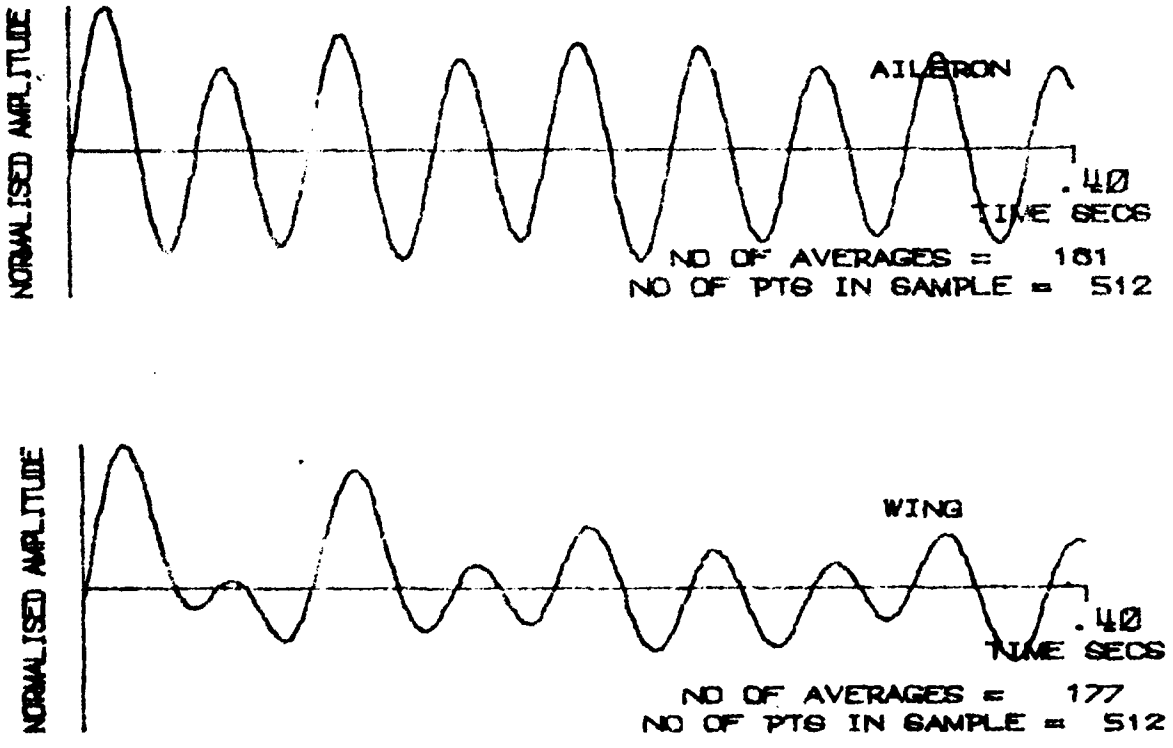

FIG.20(c) RANDOM DECREMENT SIGNATURE

AIRTRUK AT 175 Knots .... LOW-PASS FILTER AT 25 Hz

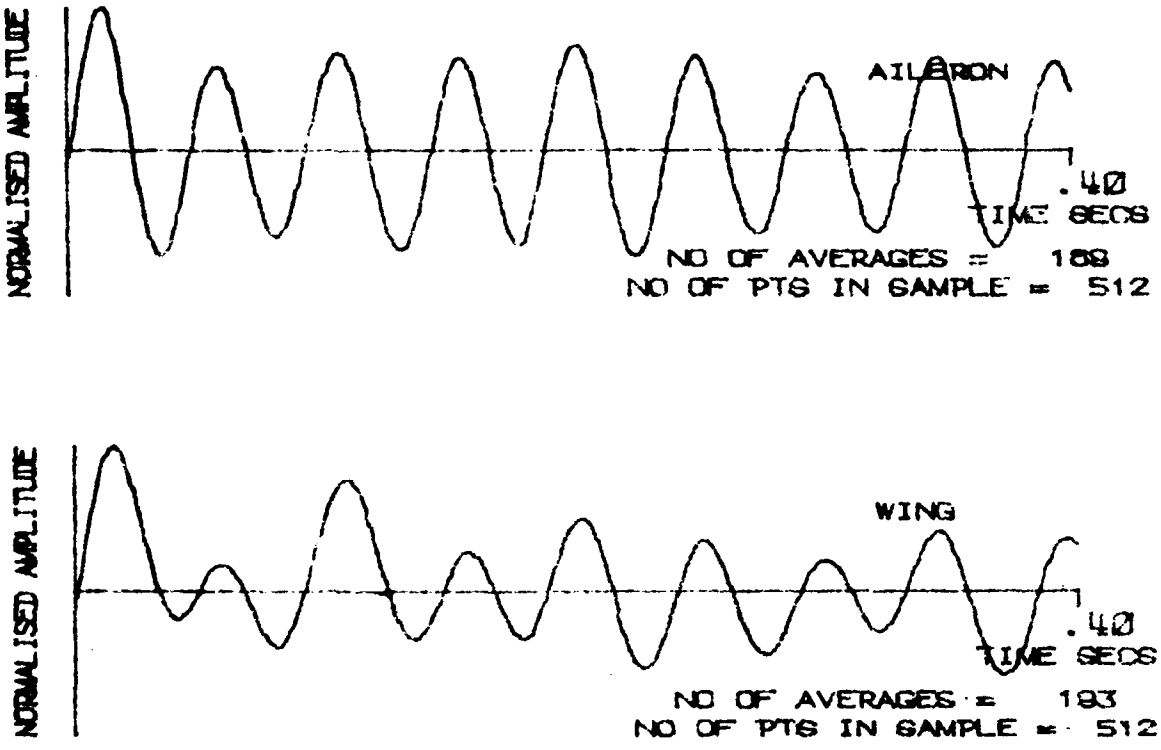

FIG.20(a) RANDOM DECREMENT SIGNATURE

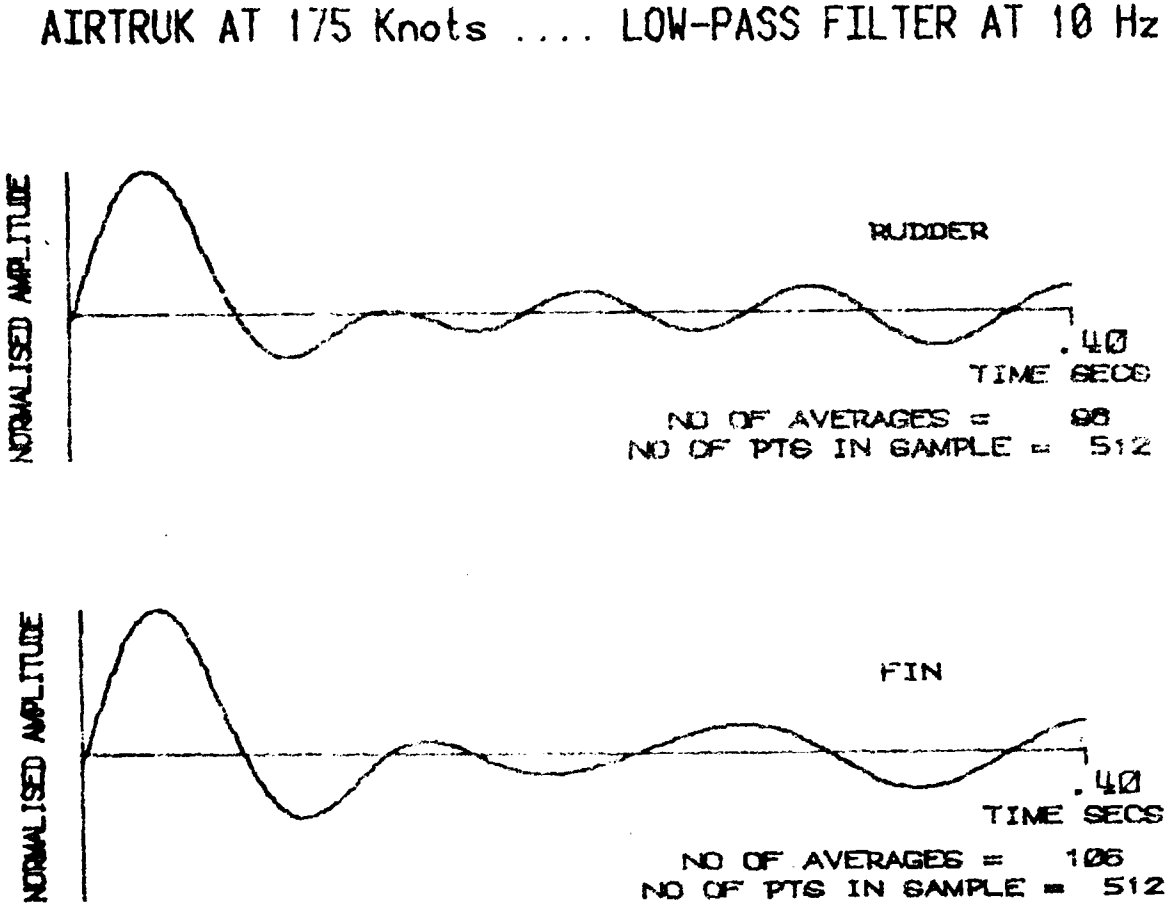

FIG.21(a) RANDOM DECREMENT SIGNATURE

AIRTRUK AT 175 Knots .... LOW-PASS FILTER AT 15 Hz

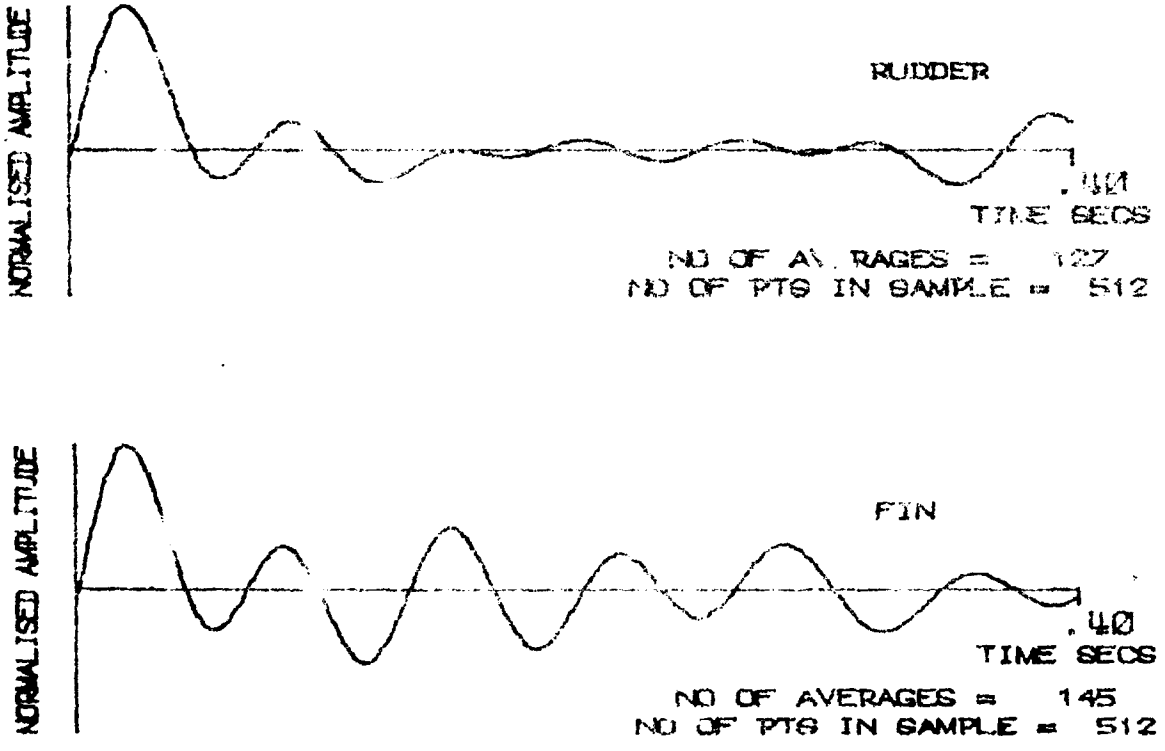

FIG.21(b) RANDOM DECREMENT SIGNATURE

AIRTRUK AT 175 Knots .... LOW-PASS FILTER AT 20 Hz

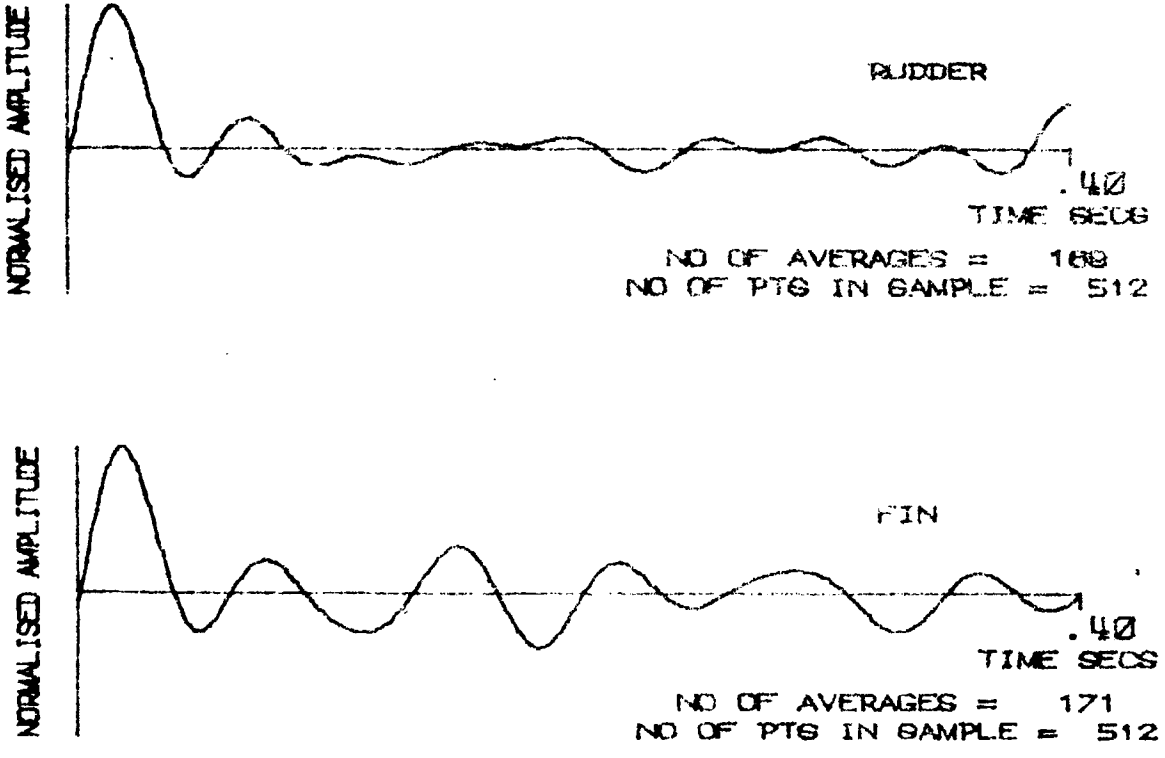

FIG.21(c) RANDOM DECREMENT SIGNATURE

AIRTRUK AT 175 Knots .... LOW-PASS FILTER AT 25 Hz

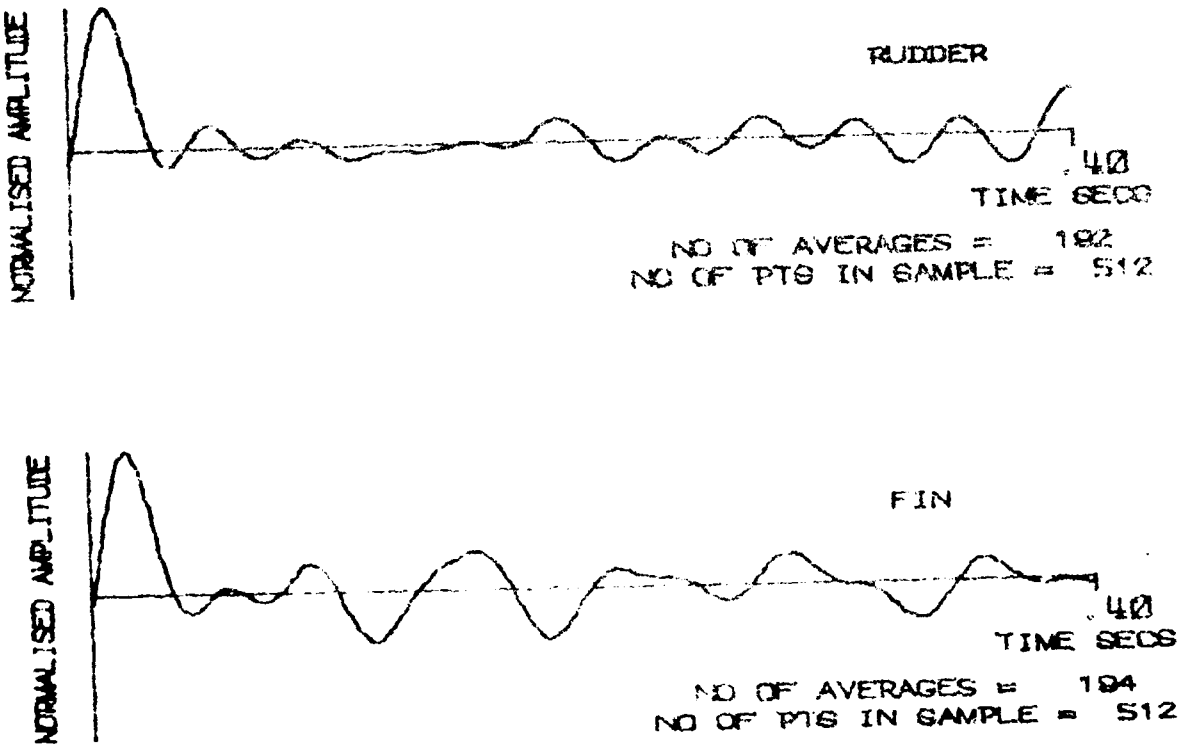

FIG.21(i) RANDOM DECREMENT SIGNATURE

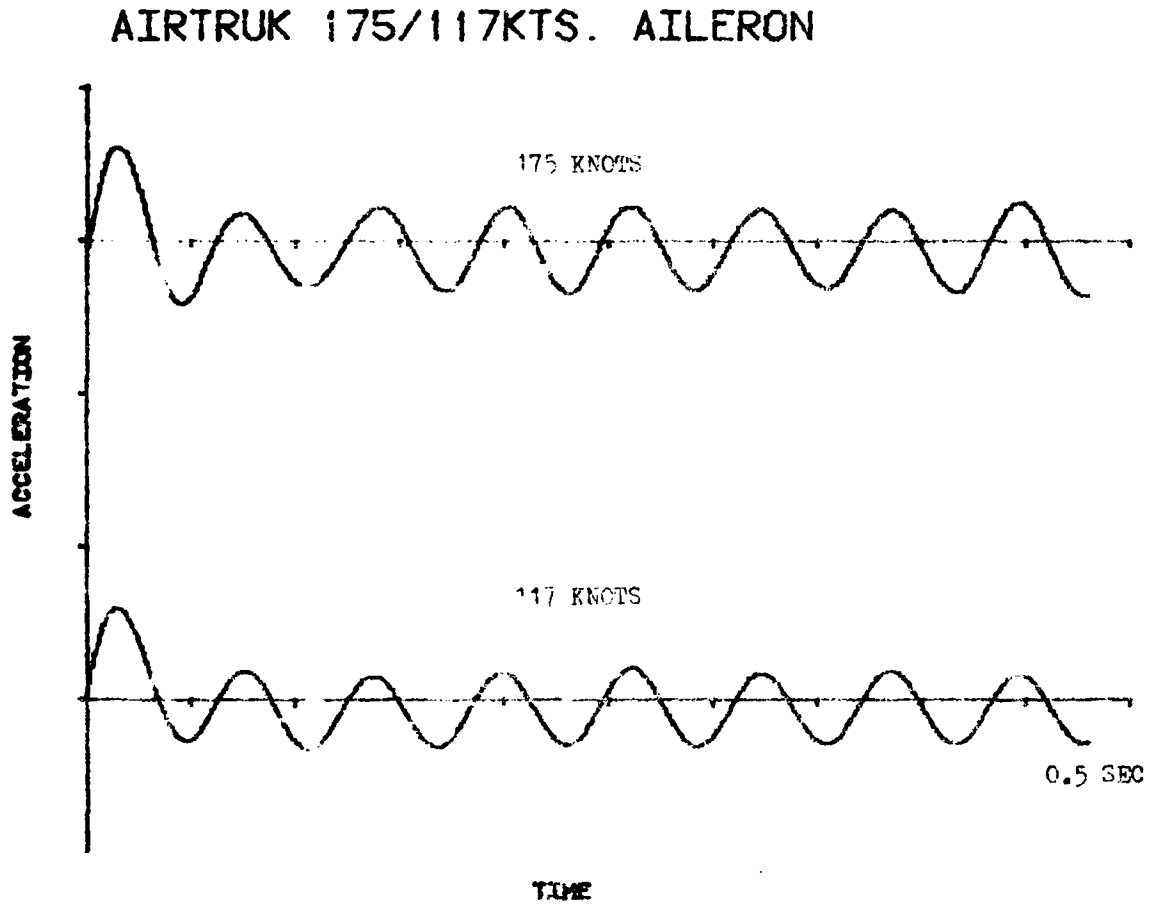

FIG.22 RANDOM DECREMENT SIGNATURES (FILTERED AT 30 HERTZ, LOW PASS)

DISTRIBUTION

AUSTRALIA

Department of Defence and Department of Defence Support

Central Office

Chief Defence Scientist)
Deputy Chief Defence Scientist)
Superintendent, Science and Technology Programmes) (1 copy)
Controller, Programmes and Analytical Studies)
Defence Science Representative (U.K.) (Doc Data sheet only)
Counsellor, Defence Science (U.S.A.) (Doc Data sheet only)
Defence Central Library
Document Exchange Centre, D.I.S.B. (17 copies)
Joint Intelligence Organisation

Aeronautical Research Laboratories

Chief Superintendent
Library
Superintendent Structures
Divisional File - Structures
Author: A. Goldman
G. Long
P. Farrell
T. Ryall
B. Emslie

Materials Research Laboratories

Library

Defence Research Centre

Library

Central Office

Director General - Army Development (NSO) (4 copies)
Defence Industry & Materiel Policy, FAS

Navy Office

Navy Scientific Adviser
Directorate of Naval Aircraft Engineering

Army Office

Army Scientific Adviser

..../cont.

Air Force Office

Aircraft Research & Development Unit
Scientific Flight Group
Library
Air Force Scientific Adviser
Technical Division Library
RAAF Academy, Point Cook

Government Aircraft Factories

Manager
Library

Department of Aviation

Library
Flying Operations and Airworthiness Division
First Assistant Secretary
Mr. M. Chandivert
Mr. M. Aubury

Statutory & State Authorities and Industry

Transavia Pty. Ltd., General Manager (2 copies)

Universities and Colleges

Adelaide	Barr Smith Library
Melbourne	Engineering Library
N.S.W.	Physical Science Library Assoc. Professor R.W.Traill-Nash, Civil Engineering
Queensland	Library
Tasmania	Engineering Library
Western Australia	Library
R.M.I.T.	Library

SPARES (4 copies)

TOTAL (65 copies)

Department of Defence

DOCUMENT CONTROL DATA

1.a AR No	1.b Establishment No	2. Document Date	3. Task No
AR-002-890	ARL-STRUC-TECH-MEMO-341	June, 1982	89/118

4. Title	5. Security	6. No Pages
FLUTTER SUBSTANTIATION TESTS ON A TRANSAVIA PL-12/T-300 AIRTRUK	a. document: UNCLASSIFIED b. title: U c. abstract: U	15 7. No Refs: 1

8. Author(s)	9. Downgrading Instructions
A. GOLDMAN	-

10. Corporate Author and Address	11. Authority (as appropriate)
Aeronautical Research Laboratories G.P.O. Box 4331, MELBOURNE, VIC. 3001	a. Sponsor b. Security c. Downgrading d. Approval -

12. Secondary Distribution (of this document)

Approved for Public Release.

Overseas enquirers outside stated limitations should be referred through ASDIS, Defence Information Services Branch, Department of Defence, Campbell Park, CANBERRA ACT 2601

13. a This document may be ANNOUNCED in catalogues and awareness services available to ...

No limitations

13. b. Citation for other purposes (ie casual announcement) may be ~~unlimited~~ unrestricted ~~or as for 13a.~~

14. Descriptors		15. COSATI Group
Fultter	Utility aircraft	2004
Flutter analysis	Airframes	0103
Aeroelasticity	Transavia Airtruk	
Vibration tests		

16. Abstract

A resonance test and subsequent flight tests have been conducted on a Transavia Airtruk. The natural modes and frequencies of vibration were measured in the ground tests, and attempts made to induce flutter during flight tests. The results of these tests are presented.

PF 65

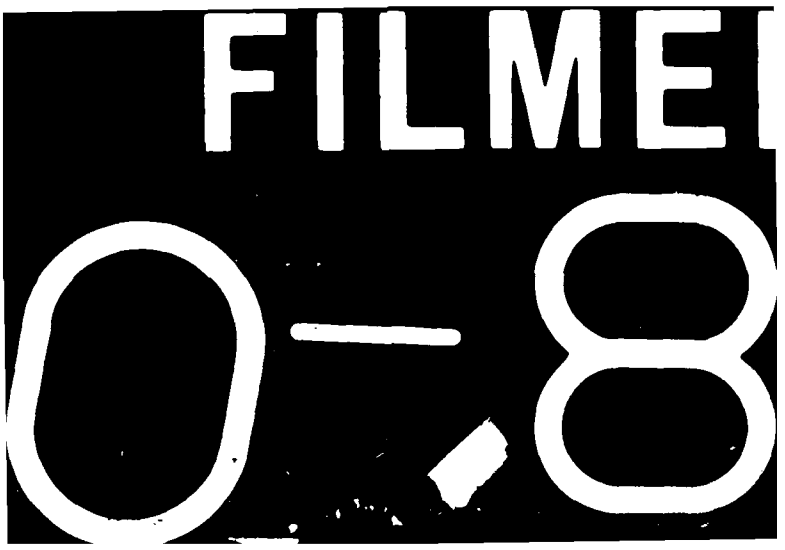
FILME
0-8